Targeting the lncRNA RBM5-AS1/GCN5 axis under fasting conditions reprograms Glycolysis and induces apoptosis in ovarian cancer cells

Article *in* Molecular Biology Reports · July 2025

DOI: 10.1007/s11033-025-10800-z

CITATIONS
0

READS
39

8 authors, including:

Gayathiri Gunasangkaran
Bharathiar University
14 PUBLICATIONS **145** CITATIONS
SEE PROFILE

Saradhadevi MUTHUKRISHNAN Saradhadevi
Bharathiar University
32 PUBLICATIONS **291** CITATIONS
SEE PROFILE

Anjali K Ravi
Bharathiar University
13 PUBLICATIONS **51** CITATIONS
SEE PROFILE

Vijay Anand
Bharathiar University
258 PUBLICATIONS **2,597** CITATIONS
SEE PROFILE

Molecular Biology Reports (2025) 52:691
https://doi.org/10.1007/s11033-025-10800-z

ORIGINAL ARTICLE

Targeting the lncRNA RBM5-AS1/GCN5 axis under fasting conditions reprograms Glycolysis and induces apoptosis in ovarian cancer cells

Gayathiri Gunasangkaran[1] · Saradhadevi Muthukrishnan[1] · Anjali K. Ravi[1] · Vijaya Anand Arumugam[2] · Velayuthaprabhu Shanmugam[3] · Kunnathur Murugesan Sakthivel[4] · Marie Arockianathan Pushpam[5] · Ashokkumar kaliyaperumal[6]

Received: 18 May 2025 / Accepted: 2 July 2025

Abstract

Background Ovarian cancer is a highly aggressive malignancy influenced by complex molecular interactions, including those involving long non-coding RNAs. RBM5-AS1, a nuclear-retained lncRNA, interacts with GCN5 to acetylate PGC-1α, thereby enhancing the Warburg effect. Although fasting is known to exert antitumor effects by modulating lncRNAs and activating PGC-1α, its impact on the RBM5-AS1/GCN5 axis in ovarian cancer remains underexplored. This study evaluates the therapeutic efficacy of RBM5-AS1 knockdown and GCN5 inhibition under fasting-mimicked conditions in SKOV3 cells.

Methods and results The findings of cytotoxicity assays revealed a dose-dependent decrease in cell viability, with the fasting + siRNA + MB-3 combination showing the most potent anticancer effect. LDH assays confirmed enhanced membrane damage in this group. Migration assays demonstrated reduced motility, while DAPI and acridine orange/ethidium bromide staining indicated significant apoptotic features present in fasting + siRNA + MB-3-treated ovarian cancer cells. Colony formation was markedly inhibited under the combination treatment, confirming suppression of clonogenic potential. Flow cytometry analysis revealed > 80% late apoptotic/necrotic cells in the fasting + siRNA + MB-3 group. Gene expression analysis further showed downregulation of Warburg-related genes (PDK1/2/3/4, LDH, GLUT1/3/4) and upregulation of PDH and pro-apoptotic markers (Caspase, Bax), alongside reduced PGC-1α acetylation.

Conclusion These findings indicate that fasting enhances the therapeutic effect of RBM5-AS1 knockdown and GCN5 inhibition, leading to a significant disruption of glycolytic metabolism and promoting apoptosis. This combinatorial approach highlights a promising metabolic and epigenetic strategy for ovarian cancer treatment.

Keywords Ovarian cancer · LncRNA RBM5-AS1 · GCN5 · PGC-1α acetylation · Warburg effect · Fasting

✉ Saradhadevi Muthukrishnan
saradhadevi@buc.edu.in; sribio770@gmail.com

Gayathiri Gunasangkaran
srigayathiridpm@gmail.com

Anjali K. Ravi
anjali1995akr@gmail.com

Vijaya Anand Arumugam
avahgmb@buc.edu.in

Velayuthaprabhu Shanmugam
velayuthaprabhu@buc.edu.in

Kunnathur Murugesan Sakthivel
sakthikm@psgcas.ac.in

Marie Arockianathan Pushpam
marie@sjctnc.edu.in

Ashokkumar kaliyaperumal
biotech.ashok@gmail.com

[1] Department of Biochemistry, Bharathiar University, Coimbatore, Tamilnadu, India

[2] Department of Human Genetics and Molecular Biology, Bharathiar University, Coimbatore, Tamil Nadu, India

[3] Department of Biotechnology, Bharathiar University, Coimbatore, Tamilnadu, India

[4] Department of Biochemistry, PSG College of Arts and Science, Coimbatore, Tamilnadu, India

[5] PG & Research, Department of Biochemistry, St. Josephs College of Arts & Science, Cuddalore, Tamilnadu, India

[6] Department of Agriculture and Animal sciences, Gandhigram Rural Institute Deemed University, Gandhigram 624 302, Tamilnadu, India

Published online: 09 July 2025

Abbreviations

OC	Ovarian cancer
LncRNA	Long noncoding RNA
RBM5-AS1	RNA binding motif protein 5-antisense
LUST	Luca–15–specific transcript
SIRT6	Sirtuin 6
GCN5	General Control Non-repressed 5 protein
PGC1α	Peroxisome proliferator-activated receptor γ coactivator-1α
PDK1	Pyruvate dehydrogenase kinase isozyme 1
FMDs	Fasting-mimicking diets
SIRT1	Sirtuin 1
TCGA	The Cancer Genome Atlas Program
ENCORI	The Encyclopedia of RNA Interactomes
GDC	Genomic Data Commons
MTT	3-(4,5-dimethylthiazol-2-yl)-2,5-diphenyl-tetrazolium bromide
RPIs	RNA-protein interactions
LDH	Lactate dehydrogenase
PI	Propidium Iodide

Introduction

Ovarian cancer (OC) is the third most prevalent gynecological malignancy among women worldwide, accounting for approximately 3.7% of total diagnosed cases and 4.7% of cancer-related deaths in 2020 [1]. According to the National Cancer Registry Program of India (2022), the mortality rate of OC in India (46,126) was higher than that in the USA (19,710) [2]. Despite significant progress in OC treatment, the 5-year relative survival rate has remained largely unchanged. Although conventional treatments such as chemotherapy, immunotherapy, and radiation therapy have improved patient survival rates, they often cause severe side effects, including nausea, hair loss, loss of appetite, weight loss, and immune-related complications etc. Additionally, resistance to chemotherapy and targeted drugs remains a significant challenge in many cases. To overcome these limitations, improving treatment approaches at the molecular level is essential for enhancing treatment effectiveness and combating drug resistance in ovarian cancer. Targeting specific metabolic pathways that drive OC progression could provide more effective and less toxic efficient alternatives to conventional treatments.

The metabolic shift of cancer cells toward high glucose uptake and lactate production, known as the Warburg effect, provides bioenergetic advantages for proliferation by enhancing non-oxidative ATP production and generating metabolic intermediates from glucose. In cancer cells, aerobic glycolysis contributes to chemoresistance by increasing lactate production and reducing the oxidative phosphorylation rate, thereby decreasing apoptosis [3]. In addition, apart from oncogenes, the long noncoding RNAs (lncRNAs) play a significant role in the OC tumorigenicity and metastasis through enhancing the Warburg mechanism [4]. lncRNAs are RNA molecules without protein-coding potential that play a crucial role in regulating transcription and translation processes in cancer cells [5]. RNA binding motif protein 5-antisense (RBM5-AS1) transcript or LUST (Luca–15–specific transcript) is a specific lncRNA highly expressed in various types of cancer and contributes to maintaining cancer cell stemness. LncRNA RBM5-AS1 promotes colon cancer and breast cancer progression by upregulating β-catenin in the Wnt signaling pathway [6, 7]. Additionally, RBM5-AS1 enhances the proliferation and metastasis of osteosarcoma [8], oral squamous cell carcinoma [9], and hepatocellular carcinoma [10] by regulating the miR-1285-3p/YAP1 axis and suppressing miR-132/212, respectively. Although RBM5-AS1 has emerged as a potential regulatory lncRNA, its exact contribution to Warburg effect modulation in ovarian cancer progression remains to be clarified.

Mechanistically, lncRNA RBM5-AS1 stabilizes the Sirtuin 6 (SIRT6) protein, promoting stemness and inducing DNA damage in medulloblastoma cells [11]. The overexpression of SIRT6 activates General Control Non-repressed 5 protein (GCN5, also known as KAT2A) by deacetylating its K549 residue, which subsequently enhances peroxisome proliferator-activated receptor γ coactivator-1α (PGC1α) acetylation [12]. The PGC1α is a key coactivator that serves as a central regulator of transcription for genes associated with mitochondrial biogenesis and respiration. The upregulation of mitochondrial respiratory activity driven by PGC-1α increases ROS production, leading to apoptosis and counteracting the Warburg effect [13]. Experimentally, PGC-1α was found to suppress the Warburg effect by downregulating pyruvate dehydrogenase kinase isozyme 1 (PDK1) through modulation of the WNT/β-catenin signaling pathway in hepatocellular carcinoma [14]. The acetylation of PGC-1α lysine residues by GCN5 is associated with the inhibition of PGC-1α activity [12].

Fasting and fasting-mimicking diets (FMDs) induce significant alterations in metabolic and growth factor profiles, potentially impairing cancer cell survival and adaptability. Incorporating periodic cycles of FMD has been shown to overcome drug resistance and promote sustained tumor regression [15]. Fasting consistently activates Sirtuin 1 (SIRT1), which deacetylates the PGC-1α for maintaining glucose metabolism and genes involved in mitochondrial fatty acid oxidation [16]. Fasting enhances SIRT1 protein expression, allowing it to interact with specific lysine residues of PGC-1α and deacetylate PGC-1α in an NAD+-dependent manner. Furthermore, under fasting conditions,

SIRT1 activates PGC-1α, thereby inhibiting lactate production from pyruvate [17]. Simultaneously, the activation of SIRT1 affects the GCN5 acetylation process on PGC-1α and prevents PGC-1α from deactivation [18]. Based on these findings, our research investigates whether targeting the lncRNA RBM5-AS1/GCN5 axis through fasting could stimulate the activity of PGC-1α via deacetylation, representing a potential strategy to overcome the malignant state of OC by downregulating the Warburg effect.

Materials and methods

In this research study, the SKOV3 cell line was purchased from the National Centre for Cell Science (NCCS, Pune, India). The chemicals and reagents were purchased from Thermo Fisher Scientific (USA), Himedia (Mumbai, India), etc. All chemicals and solvents used were of Molecular grade for systematic application.

Cell culture

The human OC cell line SKOV3 was cultured in a DMEM medium supplemented with 10% Fetal Bovine Serum and 1% Antibiotics, which were incubated with 5% CO_2 at 37 °C. Upon reaching 90% confluence, the media were discarded, and the cells were washed with 1X PBS. Subsequently, the cells were trypsinized with 0.25% trypsin and centrifuged at 2500 rpm for 5 min. The resulting pellets were collected and subcultured for further morphological and gene expression analysis.

Fasting-mimicked environment for SKOV3 cell lines

The SKOV3 cell line was cultured in a serum-reduced medium containing 1% antibiotics and incubated at 37 °C under 5% CO_2 to mimic fasting conditions in OC cells. Following this fasting induction, the OC cell lines will be utilized for additional morphological and gene expression studies.

In Silico analysis

To assess the interaction probability scores and potential binding sites of GCN5 within the regulatory sequences of the human lncRNA RBM5-AS1 gene, we employed bioinformatics tools including RPISeq (http://pridb.gdcb.iastate.edu/RPISeq/), Discovery Studio, and PyMol. Additionally, the acetylation sites on PGC-1α targeted by GCN5 were predicted using the GPS-PAIL tool (http://pail.biocuckoo.org/). Correlative analyses of gene expression profiles, overall survival rates, and comprehensive clinical data for OC were obtained from The Cancer Genome Atlas Program (TCGA) database (https://www.cbioportal.org/) and The Encyclopedia of RNA Interactomes (ENCORI) database (https://rnasysu.com/encori/panCancer.php). In the ENCORI database, gene expression data for various cancers were obtained from the TCGA project via the Genomic Data Commons (GDC) Data Portal. RNA-seq expression values were normalized using log2 (FPKM + 0.01).

SiRNA transfection

The siRNA transfection assay was performed to knock down lncRNA RBM5-AS1. Transfection was carried out using Lipofectamine RNAiMAX transfection reagent (Invitrogen) according to the manufacturer's protocol. siRNA-RBM5-AS1 (siRNA-RBM5-AS1 sense strand: CCTTTC ATTCTGAATTCATGTGCTT; siRNA-RBM5-AS1 antisense strand: CATTTCTCGAATCTGCACAGGGTTT) was transfected into the SKOV3 cell line at 75% confluence, and the transfected cells were incubated for 48 h at 37 °C under 5% CO_2. The transfection efficiency, estimated to be greater than 85%, was assessed through qRT-PCR by evaluating the site-specific knockdown of lncRNA RBM5-AS1 in OC cell lines and fasting-mimicked OC cell lines.

GCN5 inhibitor Butyrolactone 3 (MB-3) treatment in SKOV3 cell lines

SKOV3 cell lines were cultured at a density of 1×10^4 cells per well in 96-well plates. Following a 24-hour incubation period, the OC cell line and the fasting-mimicked OC cell line were treated with the GCN5 inhibitor MB-3 at a concentration of 100 µM, dissolved in either DMSO or DMEM media, as followed by Biel et al. (2004) and Kahl et al. (2019) [19, 20]. The treatment was carried out for 24 h under 5% CO_2 at 37 °C. The cytotoxic effect of MB-3 was assessed using cell viability and migration assays. Subsequently, the deacetylation status of the PGC-1α in OC cell line and the fasting-mimicked OC cell line treated with MB-3 was assessed through qRT-PCR analysis.

MTT assay

SKOV3 cell lines were seeded at a density of 1×10^4 cells per well in 96-well plates, with 8 replicate wells assigned to the following groups: untreated, siRNA transfected, GCN5 inhibitor MB-3 treated, siRNA + MB-3 treated, fasting mimicked, fasting mimicked + siRNA transfected, fasting mimicked + MB-3 treated, and fasting mimicked + siRNA transfected + MB-3 treated. After 24 h of incubation, the culture medium for both the OC cell line and the fasting-mimicked OC cell line was replaced with fresh medium

containing either individual or combined treatments of siRNA using Lipofectamine transfection reagent and MB-3. The cells were further incubated for 48 h under 5% CO_2 conditions. Cell viability was assessed using the MTT assay, in which cells were treated with 5 mg/mL of 3-(4,5-dimethylthiazol-2-yl)-2,5-diphenyltetrazolium bromide (MTT) and incubated at 37 °C for 3 h. After incubation, DMSO was added to dissolve the formazan crystals, and absorbance was measured at 570 nm using a microplate spectrophotometer [21]. The percentage of cell viability was calculated using the following equation: (Mean O.D. of treated cells / Mean O.D. of control cells) x 100.

LDH assay

SKOV3 cell lines and fasting-mimicked SKOV3 cell lines were treated with siRNA and MB-3 for 48 h. The LDH amount released in both untreated and treated cells was quantified using the LDH cytotoxicity assay kit (Invitrogen). Subsequently, the spontaneous and maximum release of the LDH amount was measured in a multiple reader at absorbances of 680 nm and 490 nm, respectively.

Wound scratch assay

SKOV3 cells were cultured in 6-well plates under both normal and fasting-mimicked conditions. Subsequently, a vertical wound scratch was created using a 10 µl sterile pipette tip, and cell debris was removed using 1X PBS. Following this, siRNA transfection was carried out using the Lipofectamine method. Additionally, the cells were treated with MB-3 and then incubated at 37 °C under 5% CO2 conditions for 48 h. Images were captured at three different time points (0, 24, and 48 h) using an inverted microscope. The migration area was quantified and analyzed using Image J software [22].

The relative migration ratio (RMR) of the cells was determined using the following formula:

$RMR = ([A_0 - (A_1 \text{ or } A_2)] / A_0) \times 100$.

Where A_0 – Initial scratch area; A_1 – Scratch area after 24 h of treatment; A_2 – Scratch area after 48 h of treatment.

DAPI staining

DAPI nuclear staining was performed to evaluate nuclear condensation and apoptosis. SKOV3 and fasting-mimicked SKOV3 cells were cultured and subjected to siRNA and MB-3 treatment for 48 h. Cells were then fixed with 3.5% paraformaldehyde for 10 min at room temperature, followed by two washes with 1X PBS. Subsequently, cells were stained with DAPI solution (5 µg/mL) and incubated in the dark for 5 min at room temperature. Fluorescence microscopy was used to analyze nuclear morphology, with excitation at 340 nm and emission detected at 480–500 nm. The percentage of apoptotic cells was determined by calculating the ratio of apoptotic cells to the total number of cells counted, multiplied by 100. A minimum of 250 cells per treatment group were analyzed [23].

AO/EtBr staining

SKOV3 and fasting-mimicked SKOV3 cells were cultured and exposed to siRNA and MB-3 for 48 h. Following treatment, both untreated and treated cells were fixed with 3.5% paraformaldehyde for 10 min at room temperature and washed twice with 1X PBS. The cells were then stained with a 1 mL solution containing acridine orange (5 mg/mL) and ethidium bromide (5 mg/mL) for 5 min. Finally, fluorescence microscopy was used to visualize and analyze the stained cells [24].

Colony formation assay

The colony formation assay was performed to evaluate the proliferation capability of OC and fasting-mimicked OC cell lines under different treatments. Cells were seeded in 6-well plates (500 cells/well) and incubated at 37 °C with 5% CO_2, followed by siRNA transfection and MB-3 treatment. The culture was maintained for 14 days, with the medium replaced every 2–3 days. After incubation, colonies were fixed with 4% paraformaldehyde for 20 min at room temperature and stained with 4 mg/mL crystal violet for 20 min. Excess stain was removed by washing with 1X PBS, and the plates were air-dried. The number of colonies formed in each well was quantified using a light microscope, and the data were analyzed to compare the impact of different treatments on SKOV3 cell proliferation [25].

Apoptotic analysis

For apoptosis determination, SKOV3 cells and fasting-mimicked SKOV3 cell lines (3×10^5 cells per well) were treated with siRNA and an MB-3 for 48 h. After treatment, cells from each group were collected and washed with pre-cooled 1X PBS. Then, the supernatant was discarded, and 400 µL of binding solution (10 mM HEPES, 140 mM NaCl, 2.5 mM $CaCl_2$, pH 7.4) was added to resuspend the cell pellet. Subsequently, 3 µL of Annexin V-FITC (1 mg/ml) and 3 µL of PI (1 mg/ml) were added to the suspension, followed by incubation at 2–8°C for 2–5 minutes in the dark. The percentage of apoptotic cells was analyzed using flow cytometry [26].

Real-Time PCR analysis

SKOV3 cells were treated with siRNA and MB-3 for 48 h under both fasting-mimicked and non-fasting conditions. After treatment, both untreated and treated cells were collected and pelleted by centrifugation at 7000xg for 5 min. Total RNA was isolated from the cells using an RNA isolation kit from Qiagen. mRNA was then reverse transcribed into cDNA using a cDNA Synthesis Kit from Takara. For quantitative RT-PCR, the cDNA was mixed with SYBR Green PCR Master Mix from Invitrogen and gene-specific primers. All reactions were performed in duplicate. To analyze the expression levels of lncRNA RBM5-AS1, GCN5, SIRT6, SIRT1, PGC1α, GLUT1, GLUT3, GLUT4, PDK1, PDK2, PDK3, PDK4, LDH, PDH axis, apoptotic genes Caspase 3, Caspase 9, Bax, and the anti-apoptotic gene Bcl2, qRT-PCR was performed using the primers listed in Table 1, with β-actin serving as an internal control. The relative expression levels of mRNA were calculated using the comparative CT method and the 2^-Delta Delta CT method.

Table 1 Quantitative real-time polymerase chain reaction primer sequences

qRT-PCR Primers for mRNAs	
LncRNA RBM5-AS1 - F	GCTTCAACACTGCGTGACAA
LncRNA RBM5-AS1 - R	CGTGGAATCAAATGGAGTGG
GCN5 - F	AGTATGTGGAGCAACTGTGT
GCN5 - R	TTGAAGTAGGTGAAGATGAA
SIRT6 - F	CAATCTGCTCATGCCCTACC
SIRT6 - R	CTTGCTTCTGGCTGATGTCC
SIRT1 - F	GGATTTGGTCGTATTGGGT
SIRT1 - R	GGAAGATGGTGATGGGAT
PGC1α - F	TTCTGCAAAAGAGAGCTTC
PGC1α - R	ATTGCATCCGTTGCATTCTC
GLUT1 - F	GCTACTCAAGCTGATTTGAT
GLUT1 - R	GGTAGTGGCACCAGAATGG
GLUT3 - F	AAGGGAAAGGCACTGGAAGT
GLUT3 - R	TGTTTGCACCGCTTATAGCA
GLUT4 - F	TGGGATTGCAAAATGACAGA
GLUT4 - R	TTCCCCATCTTCAGGATCAA
PDK1 - F	AAACGCATTTGCCATCAC
PDK1 - R	GACCTTCAGCAGTTTACAG
PDK2 - F	AATGCTTCTGGCTGATGTCC
PDK2 - R	TGGAATGAATGTTGCTGAGT
PDK3 - F	ATGTGTAGCCTTCAATCTGC
PDK3 - R	TAGTGGCACCAGAGATCAA
PDK4 - F	TCAACACTGCGTGATTGAAG
PDK4 - R	ACGCATTTGCGAAGATGAA
LDH - F	GAGTGGAATGAATGTTGCTGGT GTC
LDH - R	CCAGGATGTGTAGCCTTTGAGT TTG
PDH - F	TGCCACCAGACTAAACTAG
PDH - R	CCCGTGCCCACAATGAGAC
Cas3 - F	TGTGAGGCGGTTGTAGAAGA
Cas3 - R	GCACACCCACCGAAAACCAG
Cas9 - F	TGCTGAGCAGCGAGCTGTT
Cas9 - R	AGCCTGCCCGCTGGAT
Bax - F	AGGGTGGCTGGGAAGGC
Bax - R	TGAGCGAGGCGGTGAG
Bcl2 - F	ATCGCTCTGTGCATGACTGAGTAC
Bcl2 - R	AGAGACAGCCAGGAGAAATCA AAC
β-actin - F	GTGGGGCGCCCCAGGCACCA
β-actin - R	CTTCCTTAATGTCACGCACGAT TTC

Statistical analysis

All quantitative data were represented as mean ± standard deviation (SD) using SPSS 21.0 software, and all experiments were executed in duplicate. Student's t-test and one-way analysis of variance (ANOVA) were employed for comparisons between two or more groups. Statistical significance was defined as a p-value of less than <0.01.

Results

The significant upregulation of the LncRNA RBM5-AS1/GCN5 axis contributes to tumor progression in OC cell lines

In this investigation, we initially aimed to investigate whether lncRNA RBM5-AS1 plays a significant role in promoting OC progression by modulating metabolic reprogramming through GCN5-mediated acetylation, thereby enhancing the Warburg effect. To evaluate this hypothesis, we analyzed transcriptomic data from the TCGA database, focusing on cases with elevated RBM5-AS1 expression. Our analysis revealed RBM5-AS1-overexpressing samples exhibited a significant enrichment of genes associated with metabolic regulation (Fig. 1A). Among these, the expression of GCN5 (KAT2A) was notably increased in these cases (Fig. 1B), suggesting a potential epigenetic regulatory axis between RBM5-AS1 and GCN5 that may underlie the metabolic adaptations observed in OC cells. Although overall survival did not significantly differ between high and low RBM5-AS1 expression groups, higher RBM5-AS1 levels were associated with poorer clinical outcomes (Fig. 1C). These findings were further supported by data from the ENCORI database, which confirmed both the upregulation of RBM5-AS1 (Fig. 1D) and its positive correlation with GCN5 expression (Fig. 1E) in OC tissues.

Moreover, experimental overexpression of RBM5-AS1 in OC cell lines led to a corresponding increase in GCN5 expression, reinforcing the regulatory relationship between the genes. The expression of lncRNA RBM5-AS1/GCN5 in

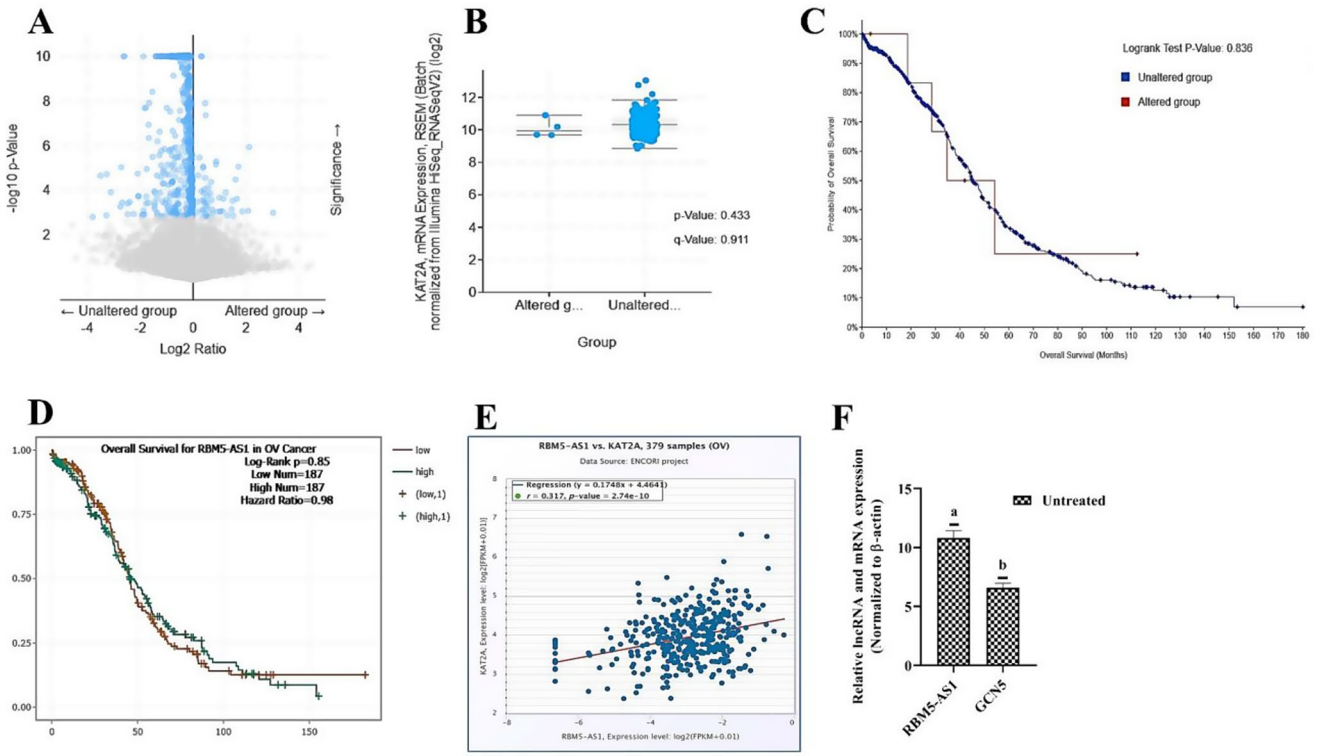

Fig. 1 RBM5–AS1–driven ovarian cancer exhibits metabolic alterations. Data reproduced from TCGA show **(A)** significantly enriched gene expression profiles (indicated in blue), including **(B)** a concurrent upregulation of GCN5 in cases where RBM5-AS1 is expressed in ovarian cancer. **(C, D)** Association between RBM5-AS1 expression levels and overall survival (OS) in ovarian cancer patients, as analyzed using data from the TCGA and ENCORI databases. **(E)** Spearman correlation analysis showing the relationship between RBM5-AS1 and GCN5 expression levels in 379 ovarian cancer tissue samples from the TCGA dataset, obtained via the ENCORI project. **(F)** The overexpression of the lncRNA RBM5-AS1/GCN5 axis in SKOV3 cell lines. Data are shown as mean ± SD based on at least two independent experiments that were statistically significant, $p < 0.05$ and $p < 0.01$. Bars with different letters are compared to each other significantly different at 5% among the treatments (LSD test)

untreated OC cell lines was quantified by Real-time PCR analysis, as shown in (Fig. 1F). RBM5-AS1, being the most substantially upregulated lncRNA, particularly caught our attention in SKOV3 cell lines. Remarkably, RBM5-AS1/GCN5 expression was upregulated in the OC cell lines with 10.8 ± 0.36 and 6.58 ± 0.22, respectively, 2^ΔCt values. The qRT-PCR results revealed a correlation between the lncRNA and GCN5 axis, modifying the metabolic signaling of ovarian cells and closely related to tumor progression.

Predicting interaction probability and putative binding sites of GCN5 on RNA-binding protein (RBP) binding sites region of LncRNA RBM5-AS1 via in-silico analysis

RNA-protein interactions (RPIs) play a crucial role in transcriptional and post-transcriptional cellular regulations. Significant interaction possibilities between lncRNA RBM5-AS1 and GCN5 were predicted by RPI-Seq analysis using both RF and SVM classifiers. Predictions with probabilities greater than 0.5 were deemed "positive," suggesting an elevated probability of a protein-lncRNA interaction. The results of the experiment showed that, with scores of 0.7 for the RF classifier and 0.98 for the SVM classifier, lncRNA RBM5-AS1 had substantial potential for interaction with GCN5 (Fig. 2A).

The lncRNA RBM5-AS1 has strong binding sites for the GCN5 acetyltransferase protein and was found using the Discovery Studio and PyMol bioinformatics prediction tools (Fig. 2B, C and D). The sequence region of lncRNA RBM5-AS1 binding sites and the amino acid regions of GCN5 were verified using NCBI data obtained with Gene ID: 100,775,107 and Uniprot ID: Q92830. The binding sites in the lncRNA RBM5-AS1 sequence from −981 bp to -1064 bp were predicted, and the interaction sequence of the GCN5 protein was found to be -496 and −658 using the PyMol tool (Fig. 2E and F). This interaction suggests that the lncRNA RBM5-AS1 binds with the GCN5 protein to enhance the activity of GCN5 in the transcriptional modification and acetylation process of PGC1α. To validate the activation of GCN5 by lncRNA RBM5-AS1, a siRNA (siRNA-RBM5-AS1 sense strand: CCTTTCATTCTGAA

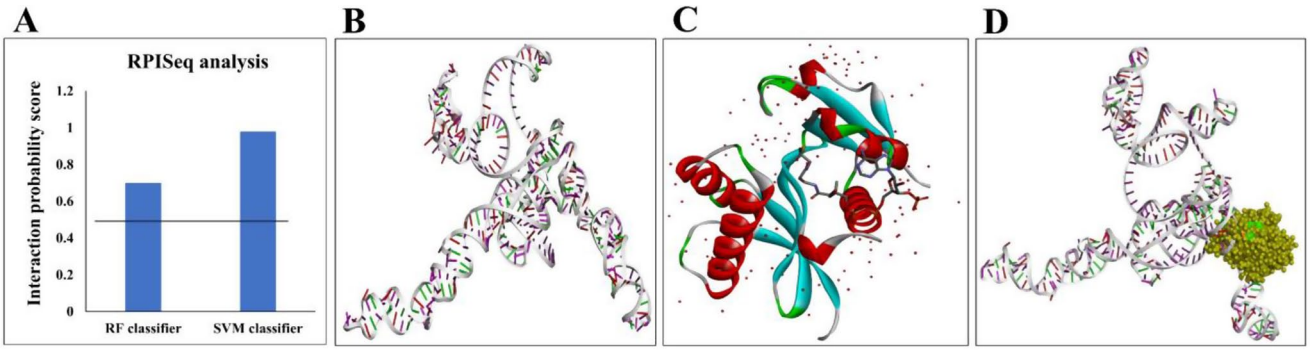

E

AAATGCCGCCACAGACTTTCACTATGTTCTCTTCACTGTCAAATGGAGAGTTTGATATACTAAGCTTACTCTCAATGGACATAATAGGAATATAA
CAAACTAGAAAAAAGGGAAACATTAAGATGTTTTAGTGATTACCAGACAGGTATTCAGTAGTTAACAAAGCCCTGCCAGGTAGGTAGCCATGT
TTAAAGGCAGAACAAATTCTATAATGAAGTCCTTGGTACTGTACTTATTCTAGTAACATCAATTTTAATATATACAAAGCTTTTTTTTTAAAAAAA
AGTCACTCCTTTGGAACAAACCACTCCTTCAACCTTTTTTTAAAATTGTACAGACTTGTTCCATTTTCATGAATATCTAGACTTGGTGAGTGAA
GCAACCTGATTGGCTTCCATCCAGCTGGTAGCATCTTGCAAGTGATAAAACTCCACGAAGGCGAAACCACGGCTTACACCTAGAGACAGCATT
CAGATATAGACGGGATACTTGTGTTAGTCAGTTCCTTTATAACAGGTGAATCTCTCTCCCACTGCTTCAACACTGCGTGACAAAGCCAATTGGG
AAGCAGCTTTACAAATGTGACTTGACTTGGGGATCTTCTTGATACTTTGCCATGGCAAGGAACAAGCCGCCTGAACTAAATGCCACTCCATTT
GATTCCACGCTTAAAGTAACCATGCAACCGACTATAGTCAAAAAAAAAAAGGAGTTTATAAATCATTACTTACCTAAGGAAAAAAAAGTCCCT
AAAACAAAGTTTAAAAAAGTTCCTCAGATGCTAACATGGTTTTCAAAGAGTCACATTCCTTAGCCATGGCAAACCTTTCATTCTGAATTCATGT
GCTTGAAGACTGGGGGAATCAGGATGTTCTTTAGGGACTGAGGTGGGAATGGGGAAGAGAACAATAATATCAGGAACTAAGCAAGCTCTCAC
CTGTTTTCCTCTTCATCAGCCTCACATCCGCAGGCTGAGGGCC**TTCGAAGGACTCCATCATTTCTCGAATCTGCACAGGGTTTTACATTAT**
TTACAGTTAAAGCTTTTGCCACACACTATTCCCCATGGAATAGGAATTACATCAACTGTTTAATTAGCCAAGTTTTTTTTTTTTTTAAGATGG
GAGTCTCTGTCTCTCACTCACTTGATTGCCCAGGCTGGAGTGCAGTGGCATGATCTCAGCTCACTGCAACCACCACCTCCTGGGTTCAAGCAA
TTCTCCTGCCTCAGCCTCCCGAGTAGCTGGGATTATAGGTGTGCACCACCATGCGTGACTGATTTTTTTTTTTTTTTGAGACGGAGTCTCGCTCT
GTCACCCAGGCTGGAGTACAGTGACGTGATCTCGGCTCACTTCAACCTCCACCTCCTGGATTCAAGCGATTCTTCTG

F

MGGGSNSSLSLDSAGAEPMPGEKRTLPENLTLEDAKRLRVMGDIPMELVNEVMLTITDPAAMLGPETSLLSANAARDETARLEER**RGIIEFHVIGN**
SLTPKANRRVLLWLVGLQNVFSHQLPRMPKEYIARLVFDPKHKTLALIKDGRVIGGICFRMFPTQGFTEIVFCAVTSNEQVKGYGTHLMNH
LKEYHIKHNILYFLTYADEYAIGYFKKQGFSKDIKVPKSRYLGYIKDYEGATLMECELNPRIPYTELSHIIKKQKEIIKKLIERKQAQIRKVYPGL
SCFKEGVRQIPVESVPGIRETGWKPLGKEKGKELKDPDQLYTTLKNLLAQIKSHPSAWPFMEPVKKSEAPDYYEVIRFPIDLKTMTERLRSRYYVTR
KLFVADLQRVIANCREYNPPDSEYCRCASALEKFFYFKLKEGGLIDK

Fig. 2 **(a)** Prediction scores of interaction possibilities between GCN5 on lncRNA RBM5-AS1 RBP sites. **(b)** Structure of lncRNA RBM5-AS1. **(c)** Structure of GCN5. **(d)** GCN5 acetyltransferase protein binding region in lncRNA RBM5-AS1 identified by Discovery Studio. **(e)** GCN5 binding sequence region in lncRNA RBM5-AS1. **(f)** The interaction region of lncRNA RBM5-AS1 in GCN5

TTCATGTGCTT; siRNA-RBM5-AS1 antisense strand: C ATTTCTCGAATCTGCACAGGGTTT) was designed to target the putative GCN5 binding site using the GenScript siRNA target finder tool.

LncRNA RBM5-AS1/GCN5 axis inactivates PGC1α by the acetylation process in OC cell lines

PGC-1α is regulated through acetylation and deacetylation mechanisms, which modulate its ability to initiate gene transcription. It is dynamically deacetylated and activated by SIRT1 and inhibited by GCN5. GCN5 is the histone lysine acetyltransferase, linking histone acetylation to transcriptional activation. In addition to histone proteins, GCN5 also acetylates non-histone targets such as PGC-1α, which contains multiple acetylation sites throughout its sequence. Under conditions of caloric restriction, reduced GCN5 expression results in decreased acetylation of PGC-1α, thereby modulating its activity. PGC-1α is activated by SIRT1-mediated deacetylation, likely in response to changes in cellular NAD+or NADH levels, or the NAD+/NADH ratio [27]. According to these previous study reports, the mRNA expression levels of the lncRNA/GCN5 axis, SIRT6, PGC-1α, and SIRT1 were quantified by the qRT-PCR method. Therefore, the results indicated that lncRNA/GCN5 increased by their respective 10.8±0.36 and 6.58±0.22 2^ΔCt values compared to the 2^ΔCt values of PGC-1α (0.49±0.15) and SIRT1 (0.97±0.29) in untreated groups of SKOV3 cell lines (Fig. 3A). These findings were further supported by data from the ENCORI database, which confirmed the upregulation of RBM5-AS1 and its positive correlation with GCN5 expression. This interaction appears to interfere with the expression of PGC-1α and SIRT1, while also indicating that RBM5-AS1 may enhance SIRT6 activity, thereby promoting increased activation of GCN5 in OC tissues (Fig. 3B, C and D). Additionally, the respective acetylation sites in PGC-1α by GCN5 were identified by the GPS-PAIL bioinformatics prediction method.

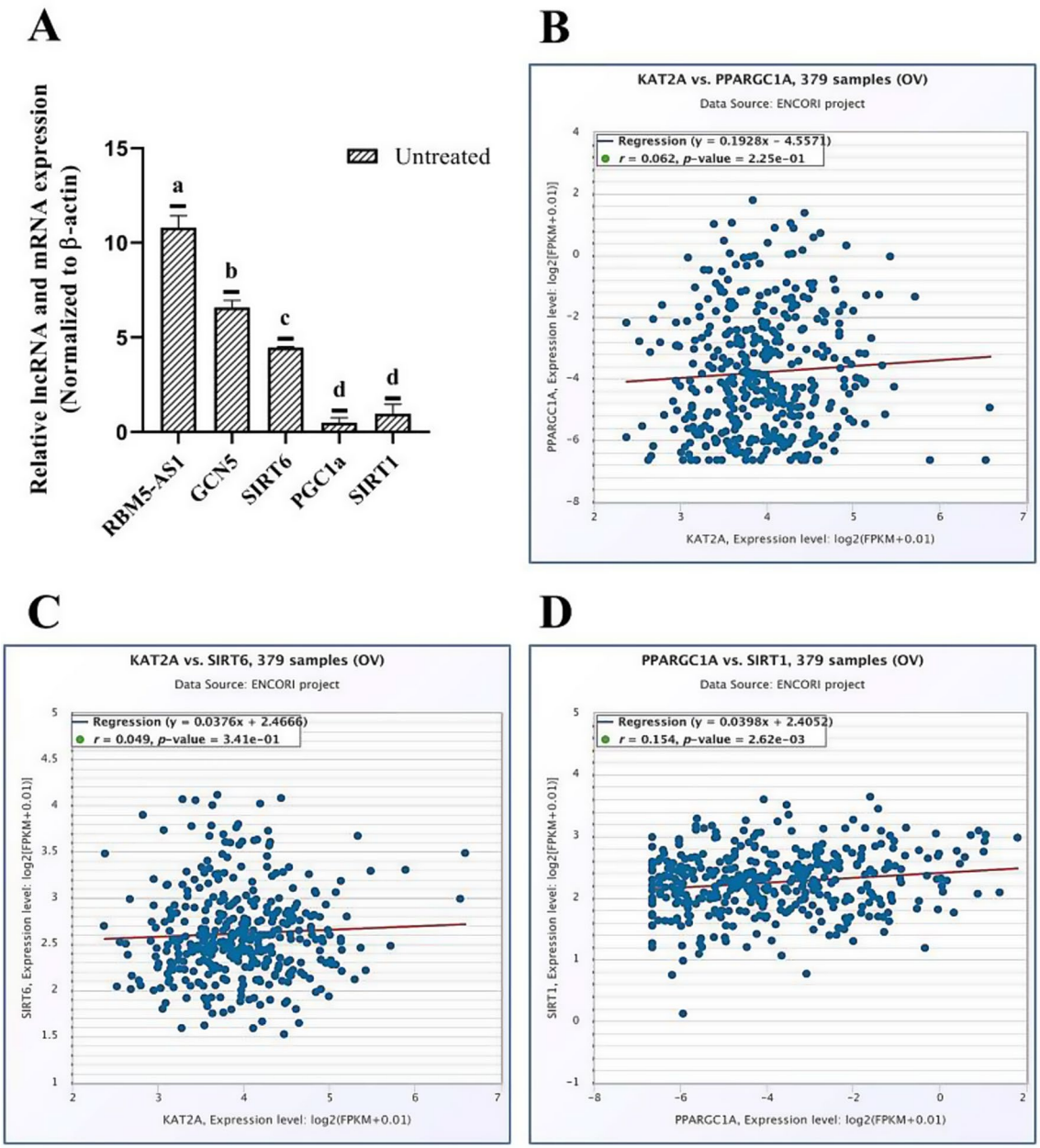

Fig. 3 LncRNA RBM5-AS1/GCN5 axis suppresses PGC-1α activity via acetylation mechanisms. **(A)** Overexpression of the lncRNA RBM5-AS1/GCN5 axis in SKOV3 ovarian cancer cells upregulates SIRT6 while concurrently downregulating SIRT1 and PGC-1α expression. Data are shown as mean ± SD based on at least two independent experiments that were statistically significant, $p<0.05$ and $p<0.01$. Bars with different letters are compared to each other significantly different at 5% among the treatments (LSD test). **(B–D)** Spearman correlation analyses depicting expression relationships between **(B)** GCN5 and PGC-1α, **(C)** GCN5 and SIRT6, and **(D)** PGC-1α and SIRT1 in ovarian cancer tissues ($n=379$) based on TCGA RNA-seq data accessed via the ENCORI database

The score values ≤ 2 from prediction sites were confirmed to be PGC-1α highly acetylated by GCN5 (Table 2). All these findings suggest that, finally, the lncRNA/GCN5 axis reverses the activity of PGC-1α by acetylation and induces the tumorigenicity through the Warburg effect.

Effect of siRNA-RBM5-AS1 knockdown combined with MB-3 on cytotoxicity and proliferation efficacy of OC cell lines

The effects of siRNA-RBM5-AS1 on SKOV3 cell lines were evaluated in the cytotoxicity test by comparing the MB-3 inhibitor. Following transfection with siRNA-RBM5-AS1 and MB-3 treatment, the cells transfected with siRNA

Table 2 Predicted sequence of PGC1α acetylated peptides with amino acid residues by GCN5 lysine acetyl transferase. Acetylated lysine residues of PGC1α were shown in Bold text

S. No	Acetylation site	Peptide sequence	Acetylation Score
1	234	NRNSSRD**K**CASKKKS	1.754
2	238	SRDKCAS**K**KKSHTQP	2
3	346	QGSHST**K**KGPEQSEL	1.696
4	655	EYRKEHE**K**RESERAK	1.464
5	662	KRESERA**K**QRERQKQ	2.174

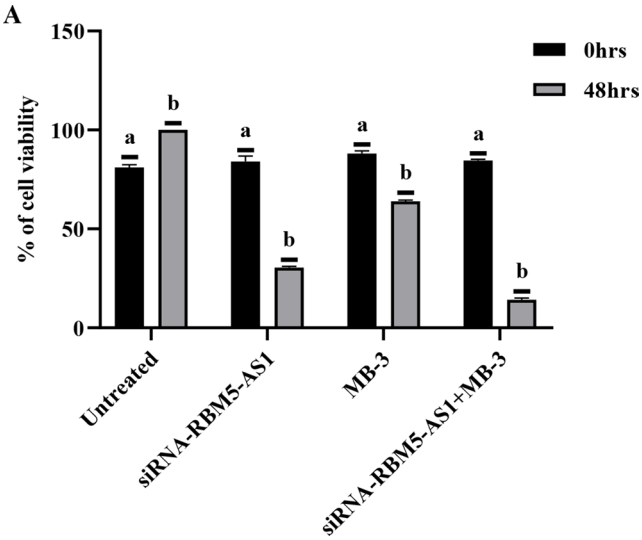

Fig. 4A The percentage of cytotoxic effect in lncRNA RBM5-AS1/GCN5 axis knockdown SKOV3 cell lines. Data are shown as mean ± SD based on at least three independent experiments that were statistically significant, $p < 0.05$ and $p < 0.01$. Bars with different letters are compared to each other significantly different at 5% among the treatments (LSD test)

exhibited more inhibitory effects than those treated with MB-3, as shown in (Fig. 4A and B). Furthermore, siRNA was combined with MB-3 to exhibit cytotoxicity observed to be above 85% compared to untreated OC cell lines. This finding implies that silencing of lncRNAs RBM5-AS1/GCN5 in OC cells prevents cancer proliferation.

The confirmation of cell inhibition percentage was further substantiated through lactate dehydrogenase (LDH) release assays, which reflect membrane damage and cytotoxicity. SKOV3 cells subjected to siRNA-mediated knockdown of the RBM5-AS1/GCN5 axis, either alone or in combination with MB-3 treatment, demonstrated varying degrees of LDH release into the culture medium after 48 h. Notably, siRNA-treated cells exhibited 68% LDH release, while MB-3-treated cells showed 55%, indicating moderate cytotoxic effects. Strikingly, the combined siRNA and MB-3 treatment resulted in the highest LDH release at 87.6%, signifying a synergistic enhancement of cell death and membrane disruption (Fig. 4C). These findings confirm that dual targeting with siRNA and MB-3 significantly compromises cancer cell integrity, supporting their combined therapeutic potential in ovarian cancer.

The scratch assay conducted on SKOV3 OC cells revealed that knockdown of the lncRNA RBM5-AS1/GCN5 axis significantly impairs cell migration and proliferation, particularly when combined with MB-3 treatment. In treated groups, the SKOV3 cells failed to migrate into the scratched area, leaving a pronounced gap even after 24 and 48 h of incubation, indicating strong inhibition of wound closure due to the knockdown process. In contrast, untreated control cells exhibited progressive closure of the wound, with the initial gap of 172 µm narrowing to 154 µm at 24 h and further to 128 µm at 48 h. However, in the siRNA-only group, the scratch gap widened from 175 µm initially to 189 µm and 203 µm at 24 and 48 h, respectively. Similarly, MB-3 alone resulted in gaps of 170 µm, 179 µm, and 190 µm, while the combination of siRNA and MB-3 maintained even larger gaps of 178 µm, 190 µm, and 205 µm at the respective time points (Fig. 4D). These results strongly suggest that silencing the RBM5-AS1/GCN5 axis markedly inhibits the migratory and invasive potential of OC cells.

DAPI staining was employed to evaluate the nuclear morphological changes associated with apoptosis in SKOV3 OC cells following siRNA-RBM5-AS1 knockdown, MB-3 treatment, and their combination. The untreated control cells exhibited intact, round nuclei with minimal fluorescence, indicating healthy nuclear morphology. In contrast, cells transfected with siRNA showed typical signs of apoptosis, such as chromatin condensation and moderate nuclear fragmentation. MB-3-treated cells exhibited similar apoptotic features, though these changes were relatively lesser extent. Remarkably, the combined siRNA and MB-3 treatment induced pronounced nuclear alterations, such as intense chromatin condensation, cell shrinkage, and distinct nuclear disintegration, characterized by strong blue fluorescence emission (Fig. 4E). These results suggest that the silencing of RBM5-AS1, particularly when combined with the GCN5 inhibitor MB-3, significantly enhances apoptotic activity in SKOV3 cells by disrupting nuclear integrity.

The treatment of SKOV3 cells with siRNA, MB-3, and the combination of siRNA + MB-3 induced significant changes in cell morphology, indicating the activation of apoptosis. Acridine orange and ethidium bromide staining revealed distinct stages of apoptosis in the treated cells. Untreated cells exhibited green fluorescence, indicating the absence of apoptosis. In contrast, cells treated with siRNA, MB-3, and siRNA + MB-3 showed yellow and reddish-orange fluorescence, which corresponded to early and late stages of apoptosis, respectively (Fig. 4F). These findings were further supported by chromatin condensation and

cellular shrinkage, which are characteristic features of apoptosis, confirming the induction of cell death in the treated groups.

Based on the apoptotic effects observed in SKOV3 cells treated with siRNA, MB-3, and the combination of siRNA + MB-3, the colony formation assay further validated the anti-proliferative impact of these treatments. The untreated control cells formed dense and numerous colonies, indicating robust proliferative capacity. In contrast, siRNA and MB-3-treated cells exhibited a marked reduction in colony number and size. Notably, the combined siRNA + MB-3 treatment demonstrated the most pronounced inhibition, with significantly fewer and smaller colonies formed, reflecting a synergistic effect in suppressing long-term cell proliferation and survival (Fig. 4G). These results underscore the efficacy of targeting the RBM5-AS1/GCN5 axis with siRNA, especially in combination with MB-3, in impairing the clonogenic potential of OC cells.

To further characterize the effects of the lncRNA RBM5-AS1/GCN5 axis on SKOV3 cells, flow cytometry measurements of apoptosis were carried out using Annexin V FITC-A and Propidium Iodide-A. Interestingly, compared to the untreated group (0.01%), the siRNA (35.6%) and MB-3 (5.33%) treated groups showed a higher percentage of early apoptotic cells. While 99.98% of cells were alive in the untreated group, the siRNA and MB-3 treated groups had live cell populations of 5.1% and 63.84%, respectively. Notably, substantial variations in the siRNA (58.75%, 0.57%) and MB-3 (15.19%, 15.64%) groups were seen in the late apoptotic/necrotic population (Fig. 4H). This finding implies that the lncRNA RBM5-AS1/GCN5 axis knockdown has increased apoptotic activity in SKOV3 cells.

Anti-proliferative and cytotoxic effects of fasting-mimicked siRNA-RBM5-AS1 knockdown combined with MB-3 on OC cell lines

The findings of the MTT experiment indicate that fasting treatment increases the cytotoxic impact of MB-3 and siRNA-RBM5-AS1 in OC cell lines. The data presented in (Fig. 5A and B) indicate that the combination of fasting with siRNA and MB-3 results in around 90% inhibition when compared to the corresponding inhibitory percentages of 38.8%, 88.9%, and 78.1% for fasting alone, fasting + siRNA, and fasting + MB-3 treated groups, respectively after 48 h incubation. This suggests that the significant reduction in OC cell viability may be mostly attributed to the silencing of lncRNA RBM5-AS1/GCN5 during fasting therapy.

The cytotoxic effect of fasting-mimicked siRNA + MB-3 was also assessed through the release of LDH into the DMEM medium, which was SKOV3 cells treated with siRNA + MB-3. The LDH release percentages from SKOV3 cell lines after 48 h of exposure to fasting alone and a combination of fasting with siRNA and MB-3 treated groups were 63.2%, 93.2%, 77.6%, and 98.6%, respectively, as mentioned in (Fig. 5C). Notably, fasting-mimicked siRNA + MB-3 elicited a higher LDH release in OC cell-treated media compared to the combination of siRNA + MB-3 without fasting, confirming that the fasting treatment induces significant cell death and reduces tumor proliferation efficacy.

The scratch assay demonstrated that the combination of siRNA transfection with MB-3 significantly reduced the migratory capacity of SKOV3 OC cells. Notably, fasting conditions further enhanced the knockdown efficiency of the lncRNA RBM5-AS1/GCN5 axis. After 24 h of incubation with fasting-mimicked siRNA + MB-3 treatment, the scratched area remained largely unhealed compared

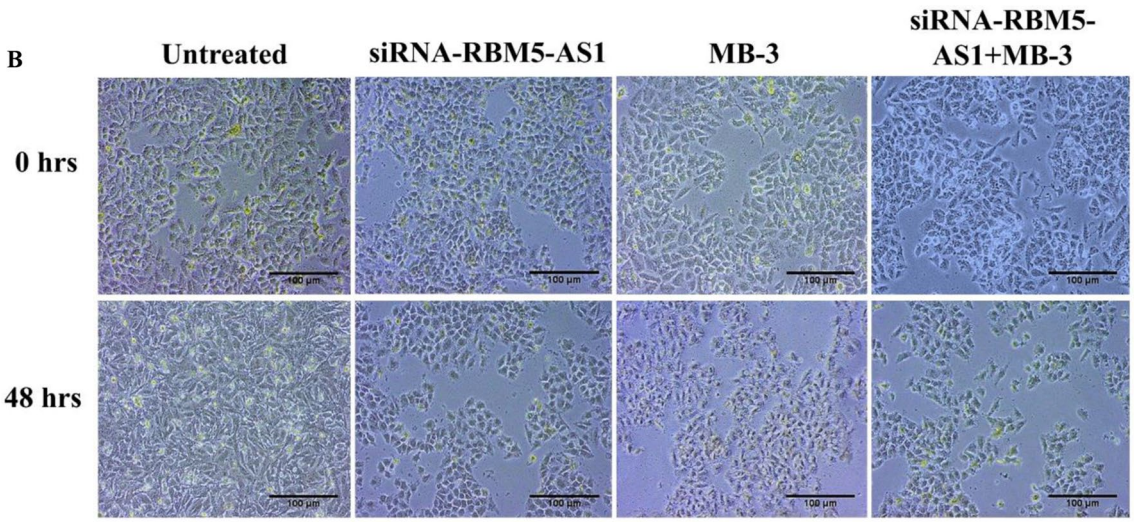

Fig. 4B Morphological representation of lncRNA RBM5-AS1/GCN5 axis knockdown SKOV3 cell lines

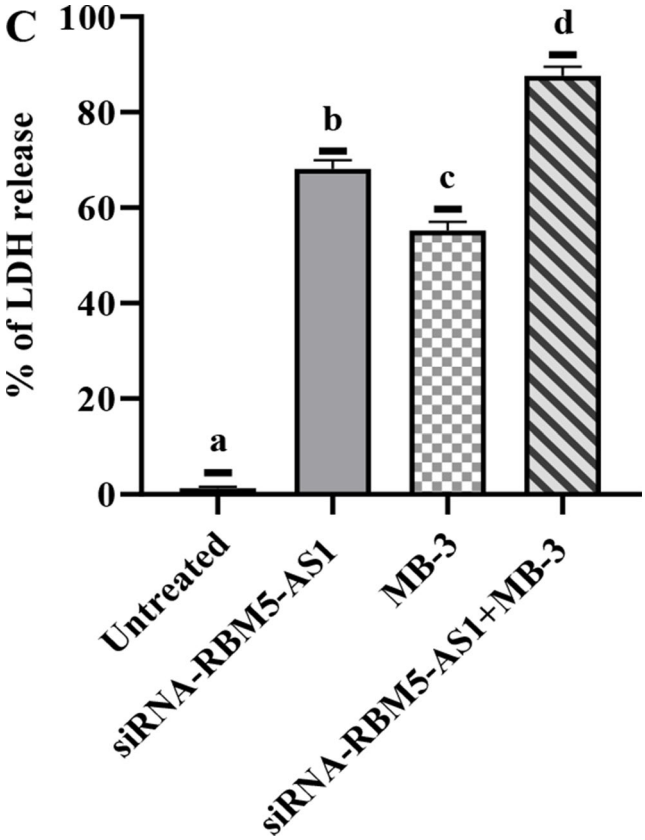

Fig. 4 C The percentage of cell membrane disruption in lncRNA RBM5-AS1/GCN5 axis knockdown SKOV3 cell lines. Data are shown as mean ± SD based on at least three independent experiments that were statistically significant, $p < 0.05$ and $p < 0.01$. Bars with different letters are compared to each other significantly different at 5% among the treatments (LSD test)

to untreated cells, indicating suppressed cellular migration. Untreated control cells exhibited approximately 34% wound closure within 48 h. In comparison, cells treated with fasting alone, fasting + siRNA, fasting + MB-3, and fasting + siRNA + MB-3 showed markedly reduced wound closure capabilities of 7.26%, 17%, 8%, and 18% at 24 h, respectively, and 13.96%, 29.4%, 16.4%, and 34.8% at 48 h (Fig. 5D). These results suggest that fasting prominently enhances siRNA + MB-3-mediated inhibition of migration by downregulating the RBM5-AS1/GCN5 axis in SKOV3 cells.

To investigate the impact of fasting on apoptosis, DAPI staining was utilized to evaluate nuclear morphology in SKOV3 OC cells after various treatments. Untreated control cells exhibited intact, structurally preserved nuclei with faint fluorescence, indicative of healthy cellular states. Cells exposed to fasting alone or fasting combined with MB-3 demonstrated early apoptotic features, including mild chromatin condensation and partial nuclear fragmentation. A more pronounced apoptotic effect was evident in the fasting + siRNA-treated group, which showed increased chromatin condensation and nuclear shrinkage. The most substantial nuclear alterations were observed in the fasting + siRNA + MB-3 group, where fragmented and condensed nuclei were prominently stained with DAPI, indicating a severe apoptotic state (Fig. 5E). These findings suggest that fasting potentiates the apoptotic effect of siRNA-mediated RBM5-AS1 knockdown and MB-3 treatment, highlighting its potential to enhance therapeutic strategies in ovarian cancer.

To assess the apoptotic effects of metabolic stress and combinatorial interventions, SKOV3 cells were subjected to acridine orange and ethidium bromide staining. Control cells predominantly exhibited green staining, indicative of viable, non-apoptotic cells. Cells exposed to fasting alone or fasting with MB-3 showed increased yellow fluorescence, reflecting induction of preliminary apoptotic changes. Fasting combined with siRNA-RBM5-AS1 further elevated apoptotic activity, as evidenced by a greater proportion of cells displaying both yellow and reddish-orange signals, corresponding to early and late apoptosis, respectively. The most pronounced apoptotic response was observed in the fasting + siRNA + MB-3 group, where intense reddish-orange staining indicated extensive progression to late apoptosis or secondary necrosis (Fig. 5F). These data demonstrate that fasting sensitizes OC cells to siRNA-mediated knockdown and epigenetic inhibition, markedly enhancing apoptotic efficacy.

Fasting potentiates the anti-proliferative effects of siRNA-RBM5-AS1 and MB-3 in SKOV3 cells. The impact of treatment on clonogenic survival under nutrient-restricted conditions was evaluated using a colony formation assay. Untreated SKOV3 cells displayed robust colony-forming ability, whereas fasting alone moderately reduced colony density. Fasting combined with MB-3 or siRNA-RBM5-AS1 individually resulted in further attenuation of colony formation, indicating enhanced suppression of proliferative capacity. Notably, the triple combination of fasting, siRNA, and MB-3 elicited the strongest anti-proliferative response, as evidenced by a marked reduction in both colony number and size (Fig. 5G). These findings demonstrate that metabolic stress via fasting significantly amplifies the cytostatic and pro-apoptotic effects of RBM5-AS1 silencing and GCN5 inhibition in OC cells.

To quantitatively assess the pro-apoptotic impact of fasting in combination with siRNA-RBM5-AS1 and MB-3, SKOV3 cells were analyzed via flow cytometry using Annexin V-FITC and Propidium Iodide (PI) staining. In untreated control cells, 99.98% remained viable, with negligible early apoptosis (0.01%) and no evidence of late apoptosis or necrosis. Fasting treatment alone modestly increased early apoptosis (45%) and reduced viability to 34.9%, while 18.3% and 1.7% of cells were in late apoptotic and necrotic

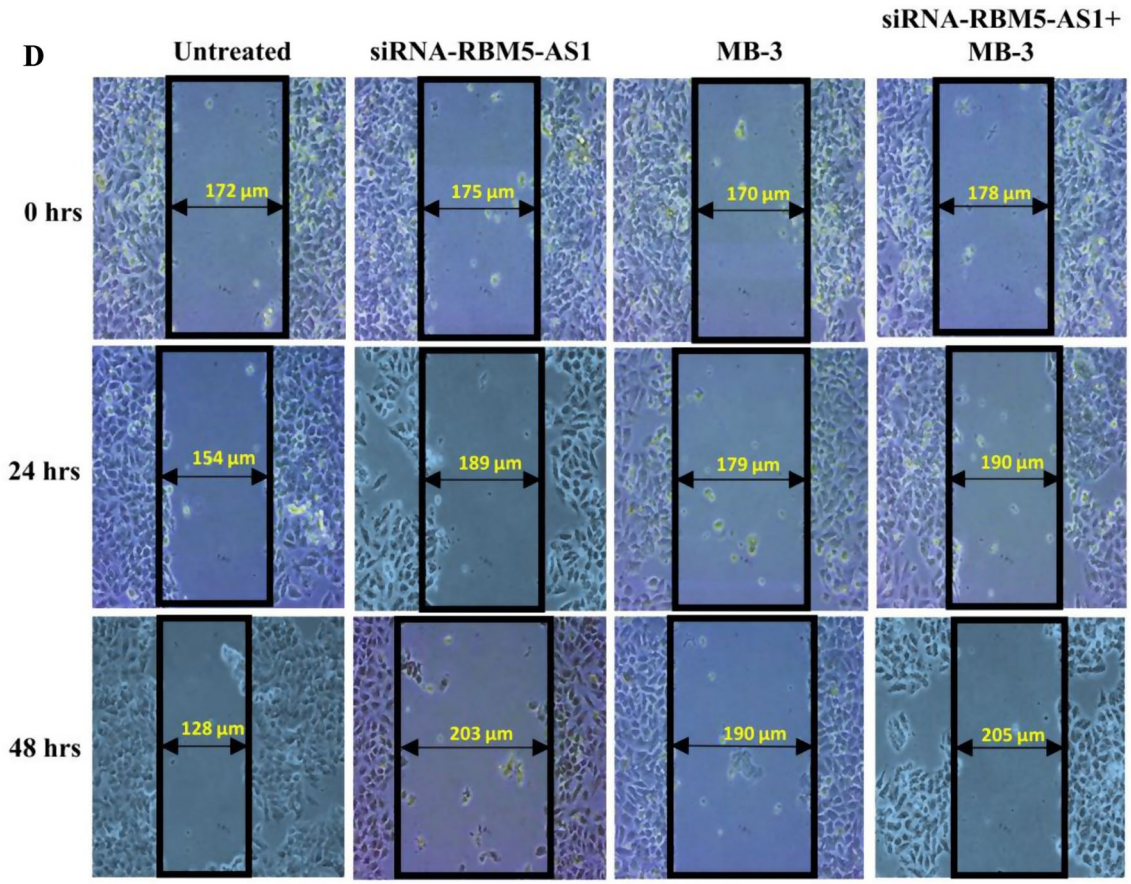

Fig. 4D Migration capability of SKOV3 cell lines under lncRNA RBM5-AS1/GCN5 axis knockdown

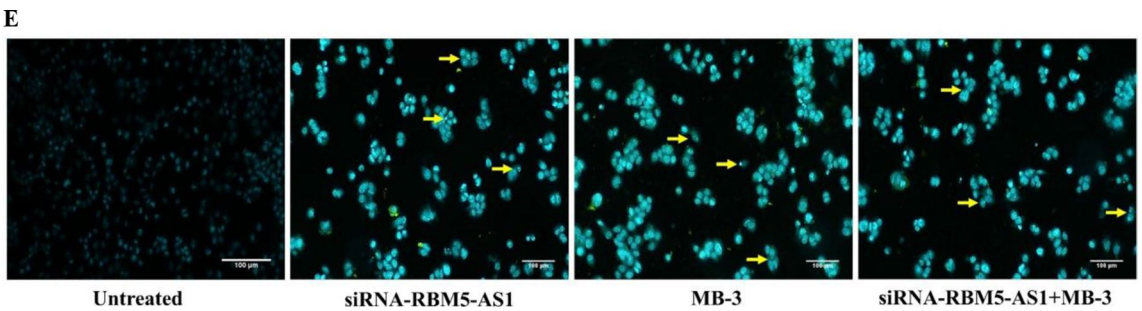

Fig. 4E Effect of siRNA+MB-3 on nuclear morphology of SKOV3 cells using DAPI staining

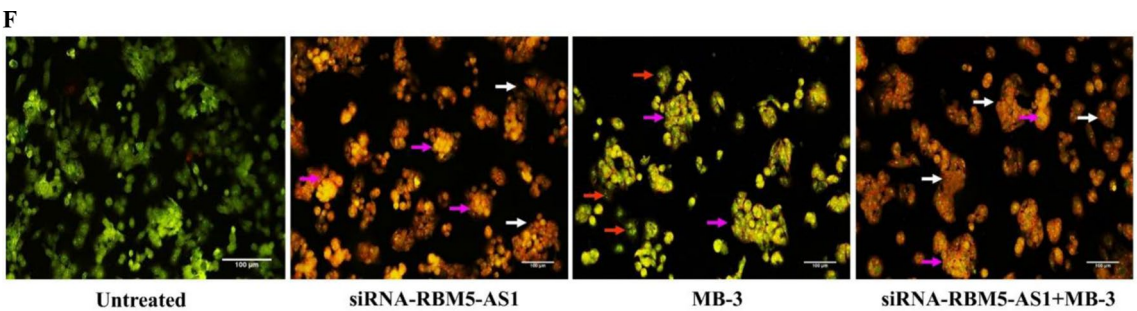

Fig. 4 F Detection of siRNA+MB-3 induced apoptosis by acridine orange and ethidium bromide staining

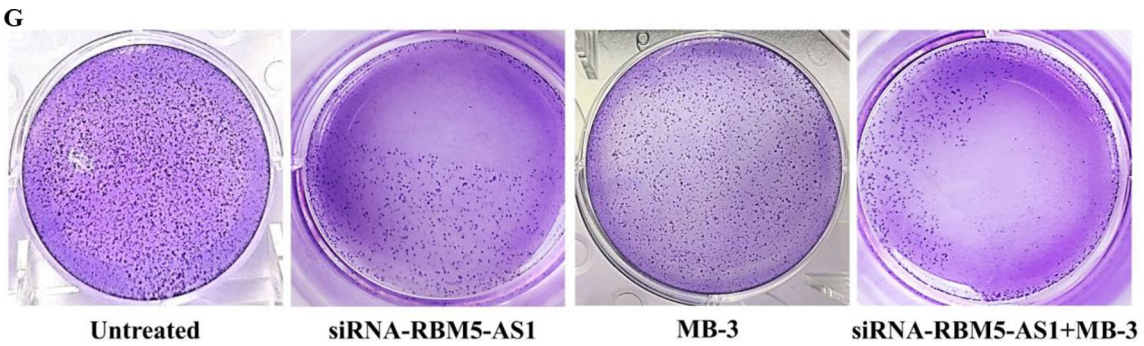

Fig. 4G Colony formation assay illustrating the anti-proliferative effects of siRNA-RBM5-AS1, MB-3, and their combination on SKOV3 ovarian cancer cells

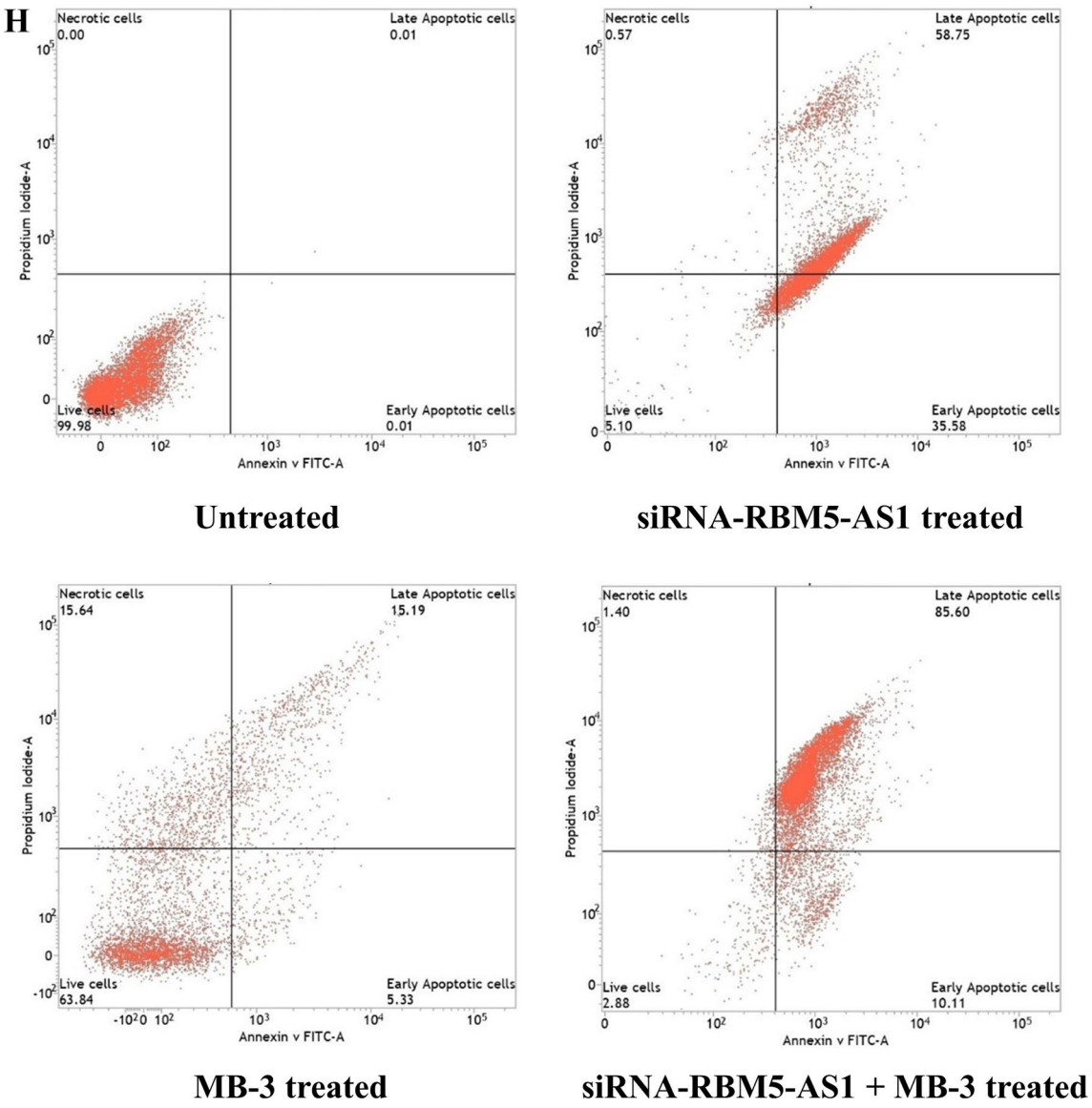

Fig. 4 H Induction of apoptotic activity in lncRNA RBM5-AS1/GCN5 axis knockdown SKOV3 cell lines analyzed by flow cytometry

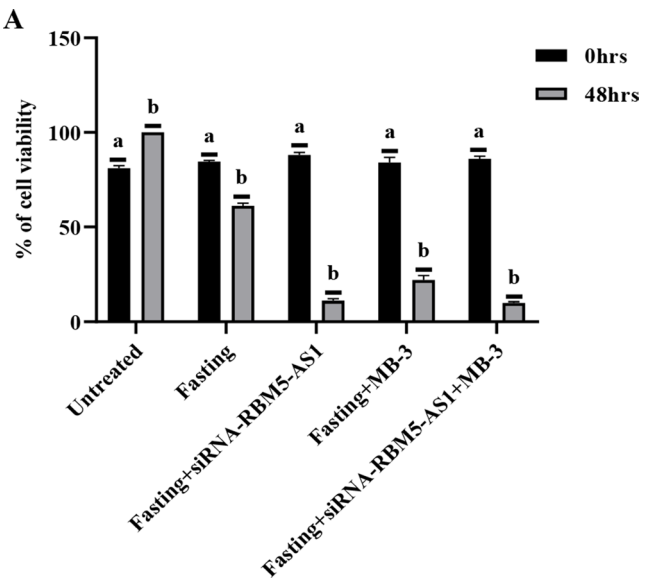

Fig. 5 A The anti-proliferative effect of fasting mimicked lncRNA RBM5-AS1/GCN5 axis knockdown in SKOV3 cell lines. Data are shown as mean ± SD based on at least three independent experiments that were statistically significant, $p < 0.05$ and $p < 0.01$. Bars with different letters are compared to each other significantly different at 5% among the treatments (LSD test)

stages, respectively. Fasting combined with MB-3 further reduced live cell populations to 29.8%, with an increase in late apoptotic (42.5%) and necrotic (4.95%) fractions. Interestingly, fasting combined with siRNA-RBM5-AS1 shifted most cells into late apoptosis (90.3%) with a minimal viable population (0.9%). The most profound apoptotic response was observed in the fasting + siRNA-RBM5-AS1 + MB-3 group, where live cells were reduced to 9.62%, early apoptotic cells accounted for 7.65%, while late apoptosis and necrosis percentages to 27.78% and 54.95%, respectively (Fig. 5H). These data underscore the enhanced apoptotic efficacy of the triple combination, suggesting that fasting significantly amplifies the impact of RBM5-AS1 silencing and GCN5 inhibition on programmed cell death in OC cells.

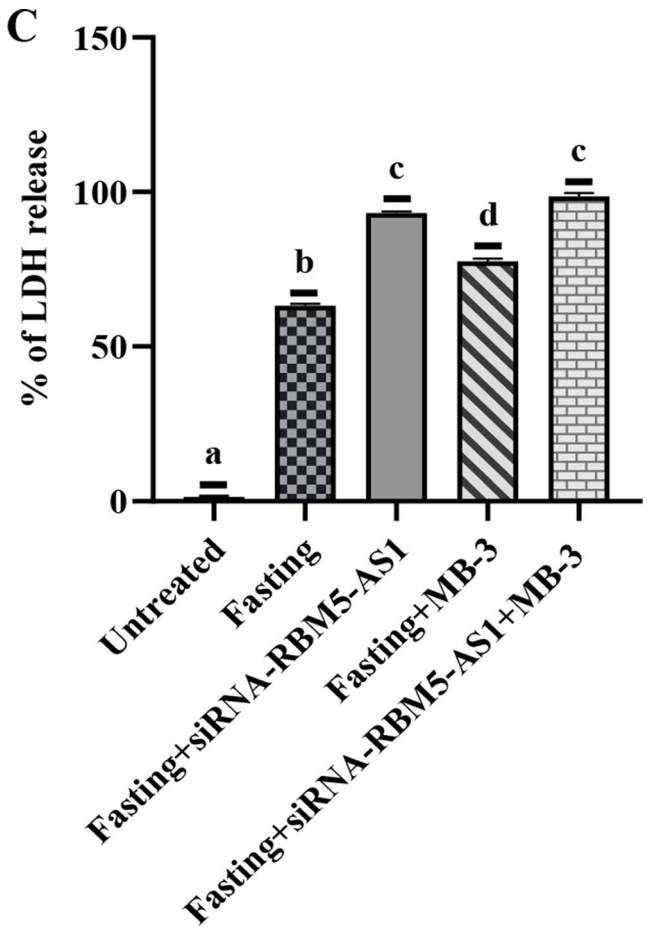

Fig. 5 C The percentage of cell membrane disruption in fasting mimicked lncRNA RBM5-AS1/GCN5 axis knockdown SKOV3 cell lines. Data are shown as mean ± SD based on at least three independent experiments that were statistically significant, $p < 0.05$ and $p < 0.01$. Bars with different letters are compared to each other significantly different at 5% among the treatments (LSD test)

Fasting-mimicked LncRNA RBM5-AS1/GCN5 axis knockdown restoring (deacetylation) the PGC1α activity in OC cell lines

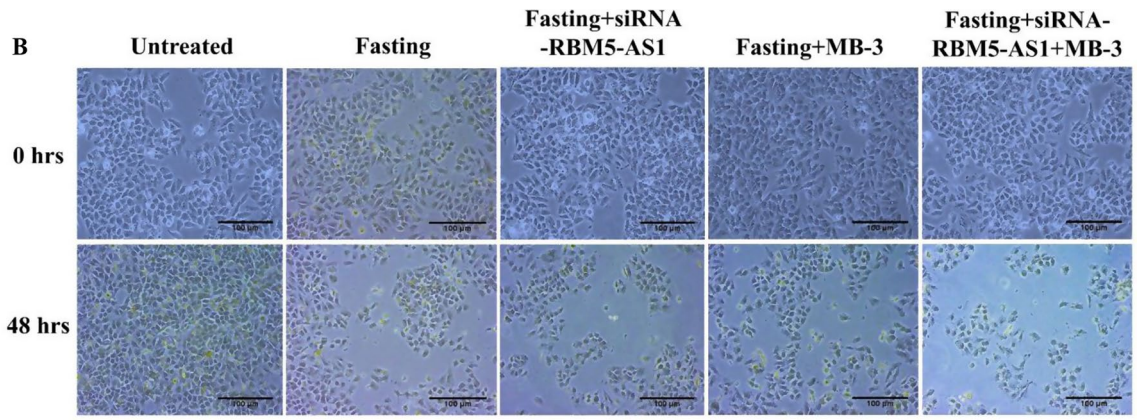

Fig. 5B Morphological changes of fasting mimicked lncRNA RBM5-AS1/GCN5 axis knockdown SKOV3 cell lines

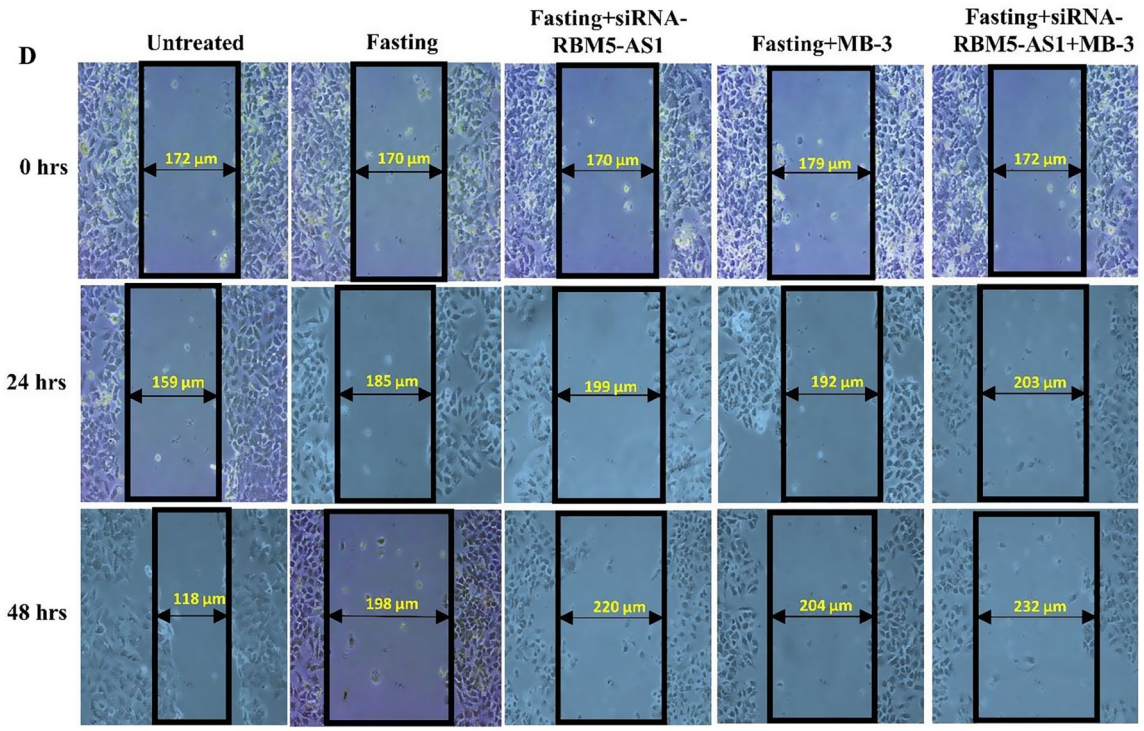

Fig. 5D Migration capability of SKOV3 cell lines under fasting-mimicked lncRNA RBM5-AS1/GCN5 axis knockdown

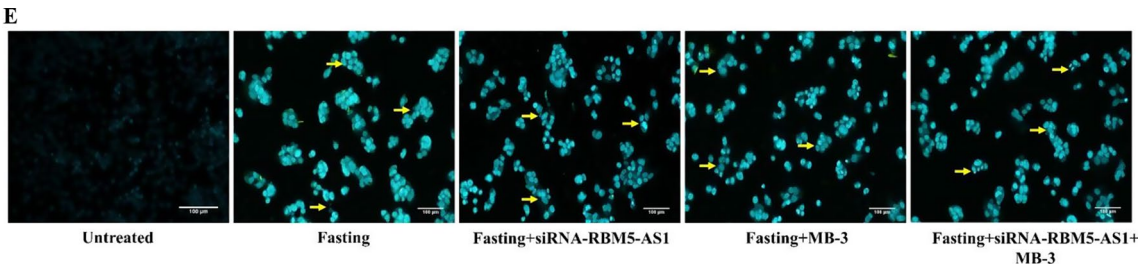

Fig. 5E Effect of fasting mimicked siRNA + MB-3 on nuclear morphology of SKOV3 cells using DAPI staining

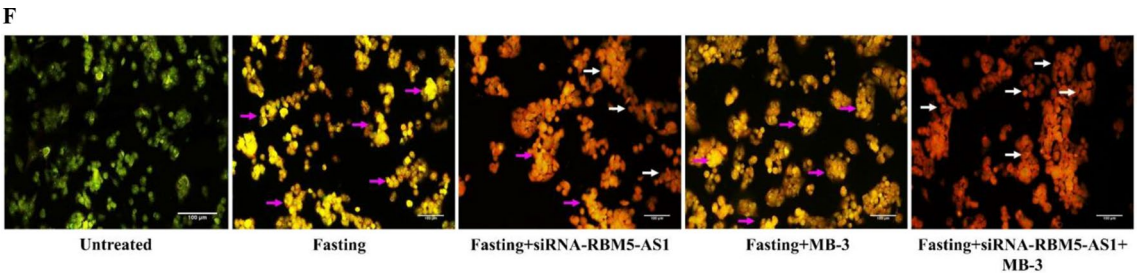

Fig. 5 F Detection of fasting-mimicked siRNA + MB-3 induced apoptosis by acridine orange and ethidium bromide staining

In order to ascertain whether GCN5 facilitated the acetylation of PGC-1α in OC cell lines, we initially investigated whether knockdown of the lncRNA RBM5-AS1/GCN5 axis through siRNA or MB-3 inhibitor would affect the levels of mRNA and protein of lncRNA RBM5-AS1/GCN5 and PGC-1α under fasting conditions. Following a 48-hour culture of SKOV3 cell lines in fasting mimicking media, along with siRNA transfection and MB-3 treatment, we observed a significant increase in the mRNA levels of SIRT1 and PGC-1α, as indicated by their respective 9.19 ± 0.32 and 7.6 ± 0.32 2^ΔCt values (Fig. 6D and E). Conversely, SIRT6 and GCN5 mRNA levels showed a decrease, as indicated by their respective 0.197 ± 0.096 and 0.43 ± 0.07 2^ΔCt values, compared to untreated cells (Fig. 6A, B and C). These

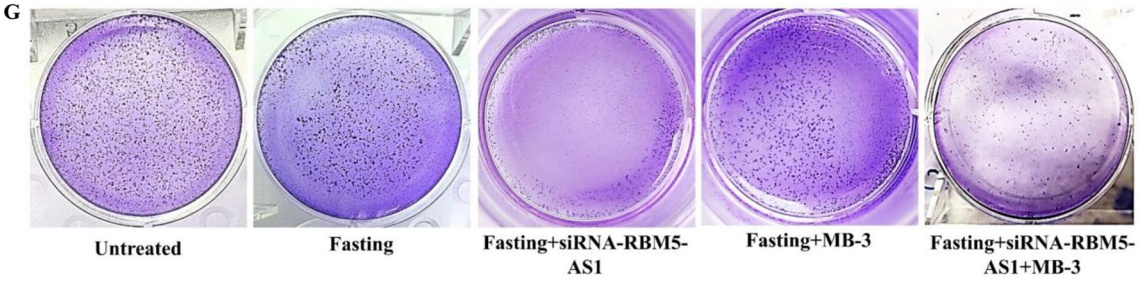

Fig. 5G Colony formation assay illustrating the anti-proliferative effects of fasting-mimicked siRNA-RBM5-AS1, MB-3, and their combination on SKOV3 ovarian cancer cells

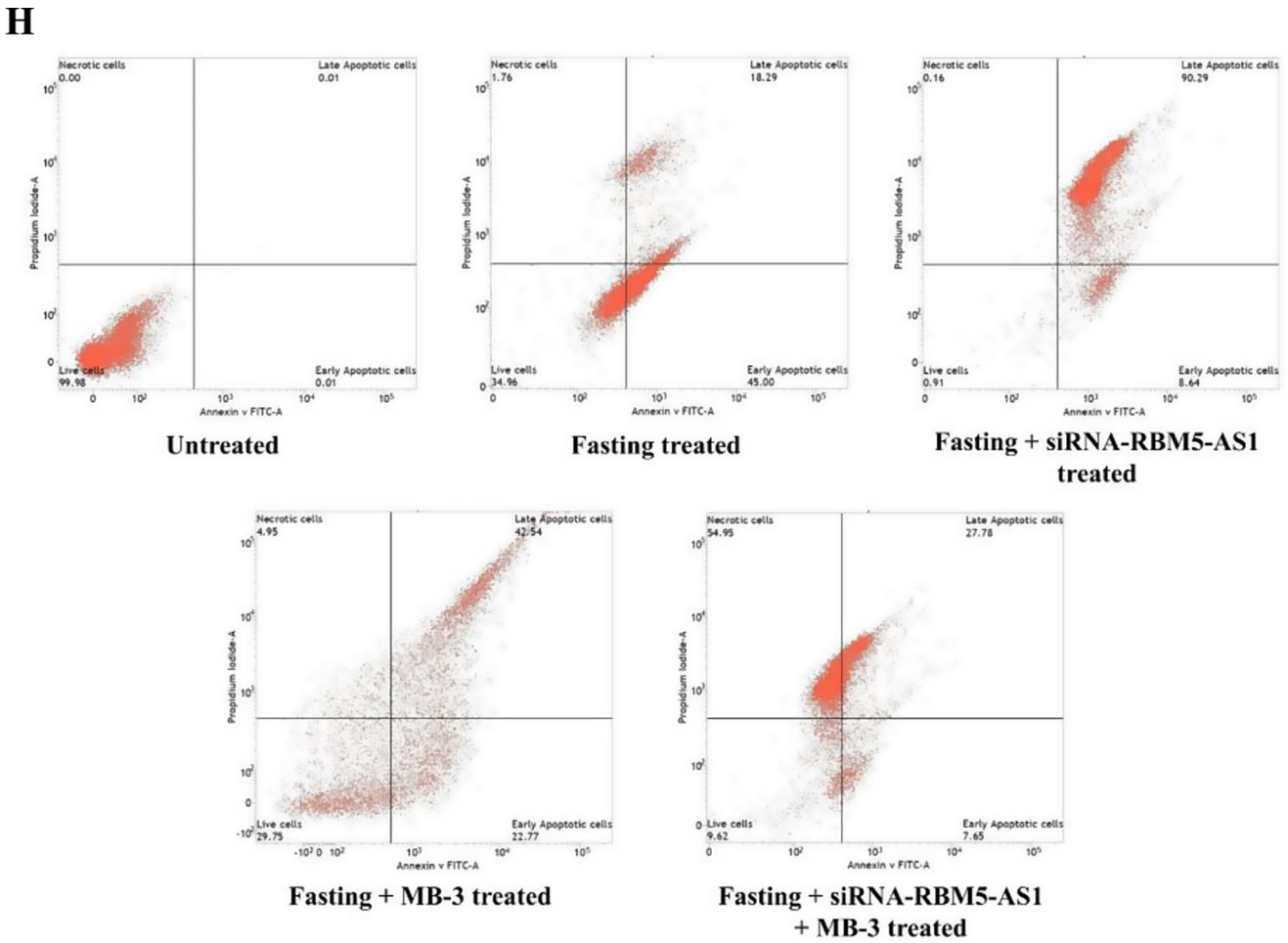

Fig. 5 H Induction of apoptotic activity in fasting mimicked lncRNA RBM5-AS1/GCN5 axis knockdown SKOV3 cell lines analyzed by flow cytometry

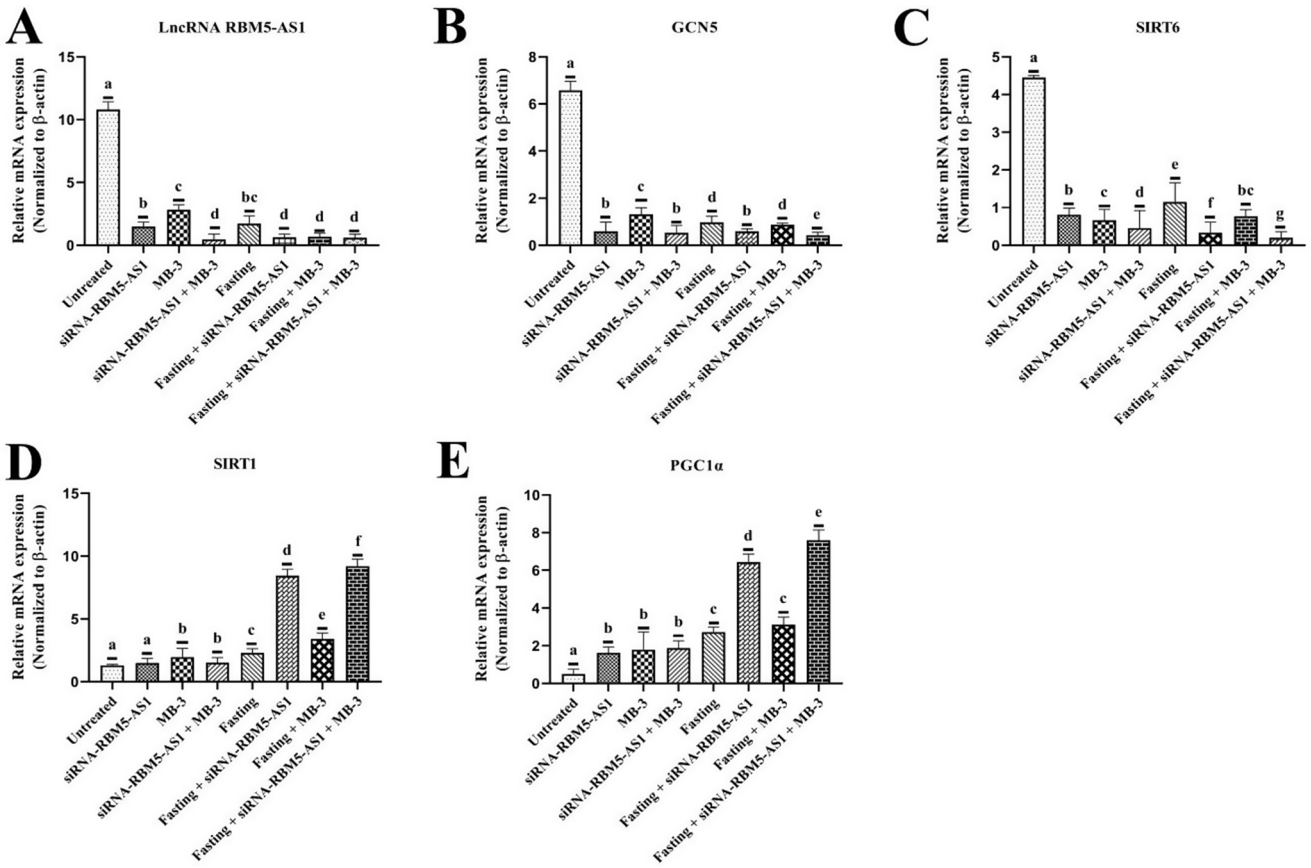

Fig. 6 Gene expression analysis of acetylation-inducing genes under fasting-mimicked LncRNA RBM5-AS1/GCN5 axis knockdown in OC cell lines. Data demonstrated mean ± standard deviation of two independent experiments is statistically significant ($p < 0.05$ and $p < 0.01$)

data demonstrated that the expression of PGC-1α is correlated with the lncRNA RBM5-AS1/GCN5 axis and SIRT6 activity.

Restoring PGC1α activity through fasting-mimicking LncRNA RBM5-AS1/GCN5 knockdown inhibits the Warburg effect and tumor progression in OC cell lines

In the regulation of PGC1α activation or deacetylation on the Warburg mechanism, we assessed the expression levels of important genes involved in tumor progression through the aerobic glycolytic pathway. Moderately, the mRNA expression levels of 9 genes (GLUT1, GLUT3, GLUT4, PDK1, PDK2, PDK3, PDK4, LDH, PDH) were quantified using real-time PCR, and the observed results indicated that the expression levels of genes show a significant low-level expression in fasting-mimicked lncRNA RBM5-AS1/GCN5 knockdown SKOV3 cell lines compared to the untreated group.

The important glycolytic markers, glucose transporters GLUT1, GLUT3, and GLUT4, show drastic decreases in their gene expression levels in lncRNA RBM5-AS1/GCN5 knockdown conjugated with fasting-treated groups (0.03 ± 0.006, 0.23 ± 0.03, and 0.20 ± 0.04-fold, respectively) (Fig. 7A, B and C). PDK isoforms facilitate metabolic switches of cancer cells by phosphorylating PDH to induce lactate production via the LDH enzyme [28]. Additionally, prior reports underline the enhanced activity of PGC1α affecting the expression levels of PDK1 in HCC cells [14]. In this context, we found that the results from qRT-PCR show that deacetylation of PGC1α via lncRNA RBM5-AS1/GCN5 knockdown through siRNA + MB-3 with fasting treatment attenuates the expression levels of PDK1, PDK2, PDK3, PDK4, and LDH with respective fold changes of 0.06 ± 0.02, 0.18 ± 0.01, 0.24 ± 0.04, 0.18 ± 0.05 and 0.25 ± 0.01 (Fig. 7D, E, F, G and H). Consequently, the suppression of PDK isoforms prevents PDH phosphorylation, increases the activity of PDH by 7.66 ± 0.04 folds (Fig. 7I), and controls lactate production to reduce cancer cell energy metabolism. Hence, the findings from gene expression analysis suggest that PGC1α is a functional upstream target for the downregulation of aerobic glycolysis.

Deacetylating PGC1α enhances apoptotic genes activity in OC cell lines.

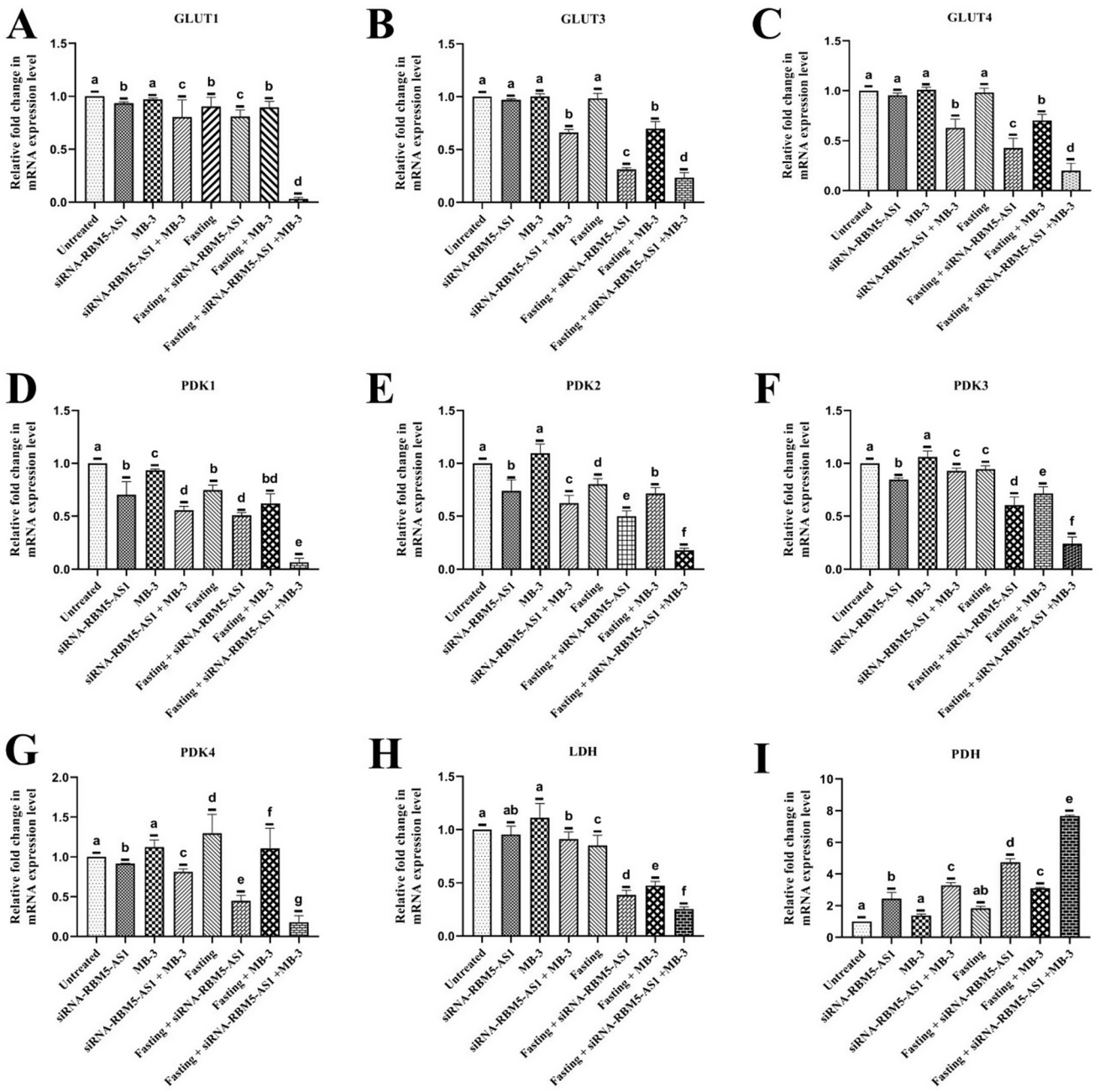

Fig. 7 Relative mRNA expression levels of glycolytic pathway genes (GLUT1, GLUT3, GLUT4, PDK1, PDK2, PDK3, PDK4, LDH, and PDH) were quantified by qRT-PCR in SKOV3 ovarian cancer cells to evaluate the impact of PGC1α activation/deacetylation on the Warburg effect. Gene expression was normalized to β-actin and presented as fold change relative to control. Data represent the mean ± SD of two independent experiments. Statistical analysis was performed using one-way ANOVA, with $p < 0.05$ and $p < 0.01$ considered significant. Bars with different letters are compared to each other significantly different at 5% among the treatments (LSD test)

The mRNA levels of the apoptotic genes Cas3, Cas9, and Bax, as well as the anti-apoptotic gene Bcl2, were measured by qRT-PCR in SKOV3 cells to further explore the impact of lncRNA RBM5-AS1/GCN5 suppression on apoptosis response. The findings show that, in comparison to untreated OC cells, there was a significant drop in the mRNA level of Bcl2 (0.17 ± 0.04 folds) (Fig. 8D) after PGC1α overexpression. However, there was a large and significant rise in the mRNA levels of the apoptotic genes Cas3 (54.6 ± 0.89 folds) (Fig. 8A), Ca9 (3.0 ± 0.24 folds) (Fig. 8B), and Bax (14.4 ± 1.2 folds) (Fig. 8C). These results validate that in SKOV3 cell lines, fasting-mimicking lncRNA RBM5-AS1/GCN5 knockdown enhances the apoptotic response by upregulating PGC1α.

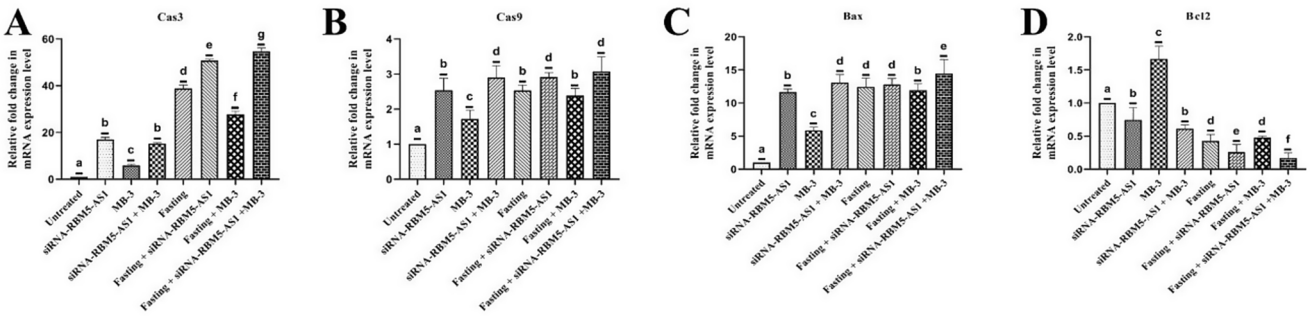

Fig. 8 Quantitative real-time PCR (qRT-PCR) analysis of the relative mRNA expression levels of pro-apoptotic genes (Caspase-3, Caspase-9, and Bax) and the anti-apoptotic gene Bcl-2 in SKOV3 ovarian cancer cells. The expression levels were measured to assess the anti-cancer effect of PGC1α modulation on apoptotic signaling pathways. Data represent the mean ± SD of two independent experiments. Statistical analysis was performed using one-way ANOVA, with $p < 0.05$ and $p < 0.01$ considered significant. Bars with different letters are compared to each other significantly different at 5% among the treatments (LSD test)

Discussion

Ovarian cancer remains one of the most challenging malignancies to treat, due to its typically silent progression and the limited availability of effective treatment options [29]. Emerging evidence underscores the pivotal role of lncRNAs in tumorigenesis, particularly in modulating metabolic pathways and gene expression [30]. Our study identifies the lncRNA RBM5-AS1 and its interaction with the histone acetyltransferase GCN5 as a novel axis regulating metabolic reprogramming in OC.

Bioinformatic analyses, alongside experimental validation, confirmed that RBM5-AS1 is upregulated in SKOV3 OC cells and is positively correlated with GCN5 expression. Molecular docking and interaction predictions through RPISeq and Discovery Studio suggested direct binding between RBM5-AS1 and GCN5, potentially enhancing GCN5's acetyltransferase activity. This interaction promotes the acetylation of PGC-1α, a central regulator of mitochondrial function and energy metabolism, thereby attenuating its activity and shifting cellular metabolism toward glycolysis, a hallmark of the Warburg effect [31, 12].

Functional assays, including cytotoxicity (MTT), LDH release, apoptosis (AO/EB, DAPI staining), and colony formation, demonstrated that RBM5-AS1 and GCN5 significantly promote OC cell viability, proliferation, and resistance to apoptosis. Notably, siRNA-mediated knockdown of RBM5-AS1, pharmacological inhibition of GCN5 via MB-3, and fasting-mimicked conditions individually exerted moderate effects, but their combination resulted in a synergistic anti-cancer response. This triple intervention induced significant cytotoxicity, enhanced apoptotic features, and markedly suppressed colony-forming ability.

Importantly, flow cytometry analyses revealed that combinatorial treatment (siRNA-RBM5-AS1 + MB-3 + fasting) led to a significant shift of OC cells into late apoptotic and necrotic populations, indicating potentiated cell death. Gene expression profiling supported these observations, with downregulation of glycolytic genes (GLUT1, GLUT3, GLUT4, PDK1-4, LDH, HIF-1α) and concurrent upregulation of apoptotic markers (Caspase-3, Caspase-9, Bax) and SIRT1, the deacetylase that counteracts GCN5's repression of PGC-1α [18, 32].

In our wound healing assay, untreated OC cells exhibited progressive closure of the wound over 48 h, indicative of high migratory capacity. In contrast, the combination of RBM5-AS1 silencing, GCN5 inhibition via MB-3, and fasting significantly impaired cell migration. Cells exposed to this treatment not only failed to close the wound but also displayed increased wound widths, suggesting suppressed motility and potential cytotoxic effects. These findings align with the observed decrease in colony formation and viability, highlighting the combined strategy's effectiveness in restricting the invasive properties of OC cells.

Mechanistically, these findings align with recent studies showing that GCN5-mediated acetylation of PGC-1α promotes glycolysis while inhibiting mitochondrial function [12]. Fasting, a known metabolic stressor, enhances SIRT1 activity, restoring PGC-1α's function and shifting metabolism back toward oxidative phosphorylation [33]. Our study is the first to demonstrate the combined effect of lncRNA knockdown, epigenetic enzyme inhibition, and metabolic modulation in reversing the Warburg phenotype in OC.

The RBM5-AS1/GCN5/PGC-1α axis thus represents a critical driver of metabolic flexibility, proliferation, and survival in ovarian cancer. The repression of PDH and upregulation of PDK isoforms by this axis underscores its role in sustaining the glycolytic phenotype typical of aggressive tumors [34]. Therapeutically targeting this axis, especially under fasting-mimicked conditions, offers a promising approach to restore apoptotic sensitivity and impede tumor metabolism.

In summary, our findings establish RBM5-AS1 as a novel oncogenic lncRNA that activates GCN5 to acetylate

and inhibit PGC-1α, thereby driving the Warburg effect and supporting ovarian cancer progression. The combinatorial treatment involving siRNA-RBM5-AS1, MB-3, and fasting effectively disrupts this axis, inducing metabolic stress, apoptosis, and migration inhibition in OC cells. These insights provide a strong rationale for targeting metabolic pathways and lncRNA-protein interactions in future OC therapies.

Conclusion

This study elucidates the critical role of the lncRNA RBM5-AS1/GCN5 axis in promoting OC progression through the modulation of PGC-1α acetylation and enhancement of the Warburg effect. Our findings demonstrate that RBM5-AS1 positively regulates GCN5 activity, facilitating aerobic glycolysis and tumor cell survival. Notably, the combinatorial treatment involving RBM5-AS1 knockdown via siRNA, GCN5 inhibition using MB-3, and fasting-mimicking conditions significantly suppressed SKOV3 cell proliferation, migration, and clonogenic potential. This synergistic approach markedly induced apoptosis and reduced the expression of glycolytic genes such as GLUT, PDK isoforms, and LDH, while upregulating apoptotic markers and the deacetylase SIRT1. These results highlight the therapeutic potential of targeting the RBM5-AS1/GCN5/PGC-1α axis to disrupt metabolic plasticity in OC cells. By integrating metabolic, epigenetic, and transcriptomic insights, this study provides a novel framework for combinatorial interventions aimed at reversing tumor bioenergetics. The enhanced sensitivity of cancer cells to treatment under fasting-mimicking conditions further supports dietary modulation as a viable adjunct to molecular therapy. Collectively, our findings highlight the RBM5-AS1/GCN5 axis as a potential therapeutic target in OC and provide a lay for future translational research focused on metabolic reprogramming strategies.

Supplementary Information The online version contains supplementary material available at https://doi.org/10.1007/s11033-025-10800-z.

Acknowledgements My co-authors and I would like to express our sincere gratitude to Dr. K. M. Saradhadevi, Assistant Professor in the Department of Biochemistry, for her constant moral support and guidance throughout this research.

Author contributions Gayathiri Gunasangkaran: First author makes a sustainable contribution to the Drafting the article, conceptual designing of the whole paper, formal analysis, methodology, and submitting the final version of the article.Saradhadevi Muthukrishnan: Corresponding author makes a sustainable contribution to the intellectual input and conceptual designing of the whole paper.Anjali K. Ravi: Formal analysis, Methodology.Vijaya Anand Arumugam: Makes a sustainable contribution to the intellectual input in the paper.Velayuthaprabhu Shanmugam, Kunnathur Murugesan Sakthivel, Marie Arockianathan Pushpam, Ashokkumar Kaliyaperumal: Co-authors who might assist the corresponding author and first author to validate the article.

Funding This research did not receive any specific grant from funding agencies in the public, commercial, or not-for-profit sectors.

Data availability No datasets were generated or analysed during the current study.

Statements & declarations

Ethics approval Not applicable.

Consent to participate Not applicable.

Consent for publication Not applicable.

Competing interests The authors declare no competing interests.

References

1. Webb PM, Jordan SJ (2024) Global epidemiology of epithelial ovarian cancer. Nat Reviews Clin Oncol 21(5):389–400. https://doi.org/10.1038/s41571-024-00881-3
2. Sathishkumar K, Chaturvedi M, Das P, Stephen S, Mathur P (2022) Cancer incidence estimates for 2022 & projection for 2025: result from National Cancer registry programme, India. Indian J Med Res 156(45):598–607. https://doi.org/10.4103/ijmr.ijmr_1821_22
3. Bianchi G, Martella R, Ravera S, Marini C, Capitanio S, Orengo A, Emionite L, Lavarello C, Amaro A, Petretto A, Pfeffer U, Sambuceti G, Pistoia V, Raffaghello L, Longo VD (2015) Fasting induces anti-Warburg effect that increases respiration but reduces ATP-synthesis to promote apoptosis in colon cancer models. Oncotarget 6(14):11806–11819. https://doi.org/10.18632/oncotarget.3688
4. Xu S, Jia G, Zhang H, Wang L, Cong Y, Lv M, Xu J, Ruan H, Jia X, Xu P, Wang Y (2021) LncRNA HOXB-AS3 promotes growth, invasion and migration of epithelial ovarian cancer by altering Glycolysis. Life Sci 264:118636. https://doi.org/10.1016/j.lfs.2020.118636
5. Gao N, Li Y, Li J, Gao Z, Yang Z, Li Y, Liu H, Fan T (2020) Long non-coding rnas: the regulatory mechanisms, research strategies, and future directions in cancers. Front Oncol 10:598817. https://doi.org/10.3389/fonc.2020.598817
6. Di Cecilia S, Zhang F, Sancho A, Li S, Aguiló F, Sun Y, Rengasamy M, Zhang W, Del Vecchio L, Salvatore F, Walsh MJ (2016) RBM5-AS1 is critical for Self-Renewal of Colon cancer Stem-like cells. Cancer Res 76(19):5615–5627. https://doi.org/10.1158/0008-5472.CAN-15-1824
7. Li X, Yang J, Ni R, Chen J, Zhou Y, Song H, Jin L, Pan Y (2022) Hypoxia-induced LncRNA RBM5-AS1 promotes tumorigenesis via activating Wnt/β-catenin signaling in breast cancer. Cell Death Dis 13(2):95. https://doi.org/10.1038/s41419-022-04536-y
8. Deng B, Pan R, Ou X, Wang T, Wang W, Nie Y, Chen H (2021) LncRNA RBM5-AS1 promotes osteosarcoma cell proliferation, migration, and invasion. Biomed Res Int 2021(1):5271291. https://doi.org/10.1155/2021/5271291

9. Li C, Ye J, Zhang Z, Gong Z, Lin Z, Ding M (2020) Long non-coding RNA RBM5-AS1 promotes the aggressive behaviors of oral squamous cell carcinoma by regulation of miR-1285-3p/YAP1 axis. Biomed Pharmacother 123:109723. https://doi.org/10.1016/j.biopha.2019.109723
10. Mu JY, Tian XJ, Chen YJ (2021) LncRNA RBM5-AS1 promotes cell proliferation and invasion by epigenetically Silencing miR-132/212 in hepatocellular carcinoma cells. Cell Biol Int 45(11):2201–2210. https://doi.org/10.1002/cbin.11649
11. Zhu C, Li K, Jiang M, Chen S (2021) RBM5-AS1 promotes radioresistance in Medulloblastoma through stabilization of SIRT6 protein. Acta Neuropathol Commun 9:123. https://doi.org/10.1186/s40478-021-01218-2
12. Mutlu B, Puigserver P (2021) GCN5 acetyltransferase in cellular energetic and metabolic processes. Biochimica et biophysica acta (BBA)-Gene regulatory mechanisms. 1864(2):194626. https://doi.org/10.1016/j.bbagrm.2020.194626
13. Li D, Wang C, Ma P, Yu Q, Gu M, Dong L, Jiang W, Pan S, Xie C, Han J, Lan Y, Sun J, Sheng P, Liu K, Wu Y, Liu L, Ma Y, Jiang H (2018) PGC1α promotes cholangiocarcinoma metastasis by upregulating PDHA1 and MPC1 expression to reverse the Warburg effect. Cell Death Dis 9(5):466. https://doi.org/10.1038/s41419-018-0494-0
14. Zuo Q, He J, Zhang S, Wang H, Jin G, Jin H, Cheng Z, Tao X, Yu C, Li B, Yang C, Wang S, Lv Y, Zhao F, Yao M, Cong W, Wang C, Qin W (2021) PPARγ Coactivator-1α suppresses metastasis of hepatocellular carcinoma by inhibiting Warburg effect by PPARγ–Dependent WNT/β-Catenin/Pyruvate dehydrogenase kinase isozyme 1 Axis. Hepatology 73(2):644–660. https://doi.org/10.1002/hep.31280
15. Caffa I, Spagnolo V, Vernieri C, Valdemarin F, Becherini P, Wei M, Brandhorst S, Zucal C, Driehuis E, Ferrando L, Piacente F, Tagliafico A, Cilli M, Mastracci L, Vellone VG, Piazza S, Cremonini AL, Gradaschi R, Mantero C, Passalacqua M, Ballestrero A, Zoppoli G, Cea M, Arrighi A, Nencioni A (2020) Fasting-mimicking diet and hormone therapy induce breast cancer regression. Nature 583:620–624. https://doi.org/10.1038/s41586-020-2502-7
16. Rodgers JT, Lerin C, Gerhart-Hines Z, Puigserver P (2008) Metabolic adaptations through the PGC-1α and SIRT1 pathways. FEBS Lett 582(1):46–53. https://doi.org/10.1016/j.febslet.2007.11.034
17. Rodgers JT, Lerin C, Haas W, Gygi SP, Spiegelman BM, Puigserver P (2005) Nutrient control of glucose homeostasis through a complex of PGC-1α and SIRT1. Nature 434:113–118. https://doi.org/10.1038/nature03354
18. Dominy JE Jr, Lee Y, Gerhart-Hines Z, Puigserver P (2010) Nutrient-dependent regulation of PGC-1α's acetylation state and metabolic function through the enzymatic activities of Sirt1/GCN5. Biochimica et biophysica acta (BBA)-proteins and proteomics 1804. 81676–1683. https://doi.org/10.1016/j.bbapap.2009.11.023
19. Biel M, Kretsovali A, Karatzali E, Papamatheakis J, Giannis A (2004) Design, synthesis, and biological evaluation of a small-molecule inhibitor of the histone acetyltransferase Gcn5. Angew Chem Int Ed 43(30):3974–3976. https://doi.org/10.1002/anie.200453879
20. Kahl M, Brioli A, Bens M, Perner F, Kresinsky A, Schnetzke U, Hinze A, Sbirkov Y, Stengel S, Simonetti G, Martinelli G, Petrie K, Zelent A, Böhmer FD, Groth M, Ernst T, Heidel FH, Scholl S, Hochhaus A, Schenk T (2019) The acetyltransferase GCN5 maintains ATRA-resistance in non-APL AML. Leukemia 33(11):2628–2639. https://doi.org/10.1038/s41375-019-0581-y
21. Lü J, Zhang C, Han J, Xu Z, Li Y, Zhen L, Zhao Q, Guo Y, Wang Z, Bischof E, Yu Z (2020) Starvation stress attenuates the miRNA-target interaction in suppressing breast cancer cell proliferation. BMC Cancer 20:627. https://doi.org/10.1186/s12885-020-07118-3
22. Zhao R, Cao B, Li H, Li T, Xu X, Cui H, Deng H, Wei B (2021) Glucose starvation suppresses gastric cancer through targeting miR-216a-5p/Farnesyl-Diphosphate farnesyltransferase 1 axis. Cancer Cell Int 21(1):704. https://doi.org/10.1186/s12935-021-02416-7
23. Muthukrishnan S, Gunasangkaran G, Ravi AK, Amirthalakshmi SR, Gandhi D, Arumugam VA, Shanmugam V, Sakthivel KM, Pushpam MA, Kaliyaperumal A, Packiaraj G, Muthukrishnan A (2024) Molecular mechanism of novel PAMAM dendrimer decorated Tectona grandis and Lactobacillus plantarum nanoparticles on Autophagy-Induced apoptosis in TNBC cells. BioNanoScience 14:2940–2963. https://doi.org/10.1007/s12668-024-01532-8
24. Muthukrishnan S, Gunasangkaran G, Swaminathan H, Kilambo PL, Ravi AK, Arumugam VA, Shanmugam V, Pushpam MA, Kaliyaperumal A, Packiaraj G (2025) Analysing the apoptotic potential of green synthesized Nyctanthes arbor-tristis Chitosan nanoparticles in MDA-MB-231 and SKOV3 cell lines. Carbohydr Res 548:109344. https://doi.org/10.1016/j.carres.2024.109344
25. Weng ML, Chen WK, Chen XY, Lu H, Sun ZR, Yu Q, Sun P, Xu Y, Zhu M, Jiang N, Zhang J, Zhang J, Song Y, Ma D, Zhang X, Miao CH (2020) Fasting inhibits aerobic Glycolysis and proliferation in colorectal cancer via the Fdft1-mediated AKT/mTOR/HIF1α pathway suppression. Nat Commun 11(1):1869. https://doi.org/10.1038/s41467-020-15795-8
26. Yang J, Gao L, Wang Z, Xu Y, Jin X, Jin Q, Yu L (2024) Effects of the LncRNA NBR2 on the proliferation and autophagy of breast cancer cells under starvation conditions. Sci Rep 14(1):22624. https://doi.org/10.1038/s41598-024-72181-w
27. Qi XM, Qiao YB, Zhang YL, Wang AC, Ren JH, Wei HZ, Li QS (2023) PGC-1α/NRF1-dependent cardiac mitochondrial biogenesis: A druggable pathway of Calycosin against triptolide cardiotoxicity. Food Chem Toxicol 171:113513. https://doi.org/10.1016/j.fct.2022.113513
28. Woolbright BL, Rajendran G, Harris RA, Taylor JA III (2019) Metabolic flexibility in cancer: targeting the pyruvate dehydrogenase kinase: pyruvate dehydrogenase axis. Mol Cancer Ther 18(10):1673–1681. https://doi.org/10.1158/1535-7163.MCT-19-0079
29. Siegel RL, Miller KD, Wagle NS, Jemal A (2023) Cancer statistics, 2023. Cancer J Clin 73(1):17–48. https://doi.org/10.3322/caac.21763
30. Peng WX, Koirala P, Mo YY (2017) LncRNA-mediated regulation of cell signaling in cancer. Oncogene 36(41):5661–5667. https://doi.org/10.1038/onc.2017.184
31. Lerin C, Rodgers JT, Kalume DE, Kim SH, Pandey A, Puigserver P (2006) GCN5 acetyltransferase complex controls glucose metabolism through transcriptional repression of PGC-1α. Cell Metabol 3(6):429–438. https://doi.org/10.1016/j.cmet.2006.04.013
32. Zhang Y, Li Q, Huang Z, Li B, Nice EC, Huang C, Liuya W, Zou B (2022) Targeting glucose metabolism enzymes in cancer treatment: current and emerging strategies. Cancers 14(19):4568. https://doi.org/10.3390/cancers14194568
33. Longo VD, Panda S (2016) Fasting, circadian rhythms, and time-restricted feeding in healthy lifespan. Cell Metabol 23(6):1048–1059. https://doi.org/10.1016/j.cmet.2016.06.001
34. Anwar S, Shamsi A, Mohammad T, Islam A, Hassan MI (2021) Targeting pyruvate dehydrogenase kinase signaling in the development of effective cancer therapy. Biochimica et biophysica acta (BBA)-Reviews on Cancer. 1876(1):188568. https://doi.org/10.1016/j.bbcan.2021.188568